Inorganic Chemistry

Article

pubs.acs.org/IC

Formation of Cationic $[RP_5Cl]^+$-Cages via Insertion of $[RPCl]^+$-Cations into a P–P Bond of the P_4 Tetrahedron

Michael H. Holthausen,[†] Kai-Oliver Feldmann,[†,‡] Stephen Schulz,[†] Alexander Hepp,[†] and Jan J. Weigand*[,†]

[†]Institut für Anorganische and Analytische Chemie and [‡]Graduate School of Chemistry, Westfaelische Wilhelms Universitaet Muenster, Corrensstrasse 30, 48149 Muenster, Germany

Supporting Information

ABSTRACT: Fluorobenzene solutions of $RPCl_2$ and a Lewis acid such as ECl_3 (E = Al, Ga) in a 1:1 ratio are used as reactive sources of chlorophosphenium cations $[RPCl]^+$, which insert into P–P bonds of dissolved P_4. This general protocol represents a powerful strategy for the synthesis of new cationic chloro-substituted organophosphorus $[RP_5Cl]^+$-cages as illustrated by the isolation of several monocations (**21a-g**$^+$) in good to excellent yields. For singular reaction two possible reaction mechanisms are proposed on the basis of quantum chemical calculations. The intriguing NMR spectra and structures of the obtained cationic $[RP_5Cl]^+$-cages are discussed. Furthermore, the reactions of dichlorophosphanes and the Lewis acid $GaCl_3$ in various stoichiometries are investigated to obtain a deeper understanding of the species involved in these reactions. The formation of intermediates such as $RPCl_2{\cdot}GaCl_3$ (**14**) adducts, dichlorophosphanylchlorophosphonium cations $[RPCl_2{-}RPCl]^+$ (**16**$^+$) and $[RPCl_2{-}RPCl{-}GaCl_3]^+$ (**17**$^+$) in reaction mixtures of $RPCl_2$ and $GaCl_3$ in fluorobenzene strongly depends on the basicity of the dichlorophosphane $RPCl_2$ (R = *t*Bu, Cy, *i*Pr, Et, Me, Ph, C_6F_5) and the reaction stoichiometry.

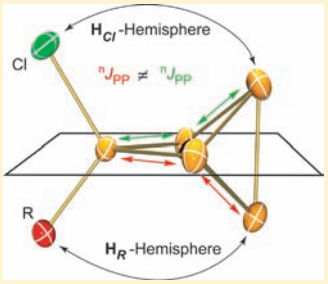

INTRODUCTION

Anionic and neutral phosphorus cage and ring compounds have been thoroughly investigated.[1] However, the diversity of cationic polyphosphorus derivatives is mostly limited to *catenated* cyclic or acyclic polyphosphanylphosphonium salts.[2]

Cationic $[P_5X_2]^+$-cages **1**$^+$ (X = Cl, Br, I) were reported only recently. Cations **1**$^+$ resulted from the reaction of the silver salt $Ag[Al\{OC(CF_3)_3\}_4]$ with PX_3 (X = Cl, Br, I) in the presence of P_4.[3] Applying a stoichiometric melt approach at elevated temperatures (60 to 100 °C),[4] we were able to extend this chemistry by intercepting the more stable diorganophosphenium cation $[Ph_2P]^+$ with P_4. This approach resulted in the formation of the cationic cages $[Ph_2P_5]^+$ (**2**$^+$), $[Ph_4P_6]^{2+}$ (**3**$^{2+}$), and $[Ph_6P_7]^{3+}$ (**4**$^{3+}$) via the consecutive insertion of up to three $[Ph_2P]^+$ into the P–P bonds of the P_4 tetrahedron (Chart 1).[5]

Chart 1. Cationic Phosphorus Cages

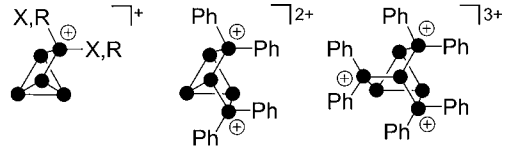

Similarly, the reaction of P_4 with the *cyclo*-diphosphadiazane $[DippNPCl]_2$ (Dipp = 2,6-diisopropylphenyl) and $GaCl_3$ in fluorobenzene yielded compound **5**$[GaCl_4]$. The addition of an excess $GaCl_3$ and a second equiv of P_4 to a solution of **5**$[GaCl_4]$ afforded the dicationic species **6**$^{2+}$ as $[Ga_2Cl_7]^-$ salt.[6] This approach has been extended to highly functionalized cation **7**$^+$ and the zwitterionic P_5-cage **8**, which are formed by the insertion of the corresponding phosphenium cations that are derived from four-membered phosphorus–nitrogen-metal heterocycles (Chart 2).[7]

Chart 2. Cationic Phosphorus Cages from Four-Membered Heterocycles

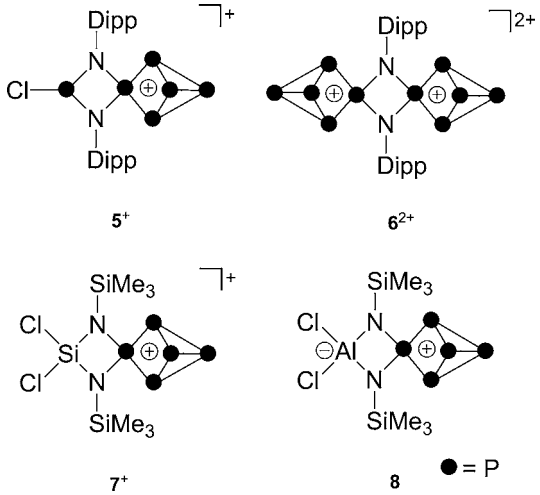

In continuation of our investigations, we became interested in protocols for the generation of functionalized P_5-cages.

Received: June 21, 2011
Published: February 28, 2012

   dx.doi.org/10.1021/ic2013304 | *Inorg. Chem.* 2012, 51, 3374–3387

Herein, we report a convenient, high yielding one-pot procedure for the preparation of a range of cationic $[RP_5Cl]^+$-cages. The reaction proceeds formally via chlorophosphenium ions $[RPCl]^+$ that are generated in situ from dichlorophosphanes and a Lewis acid ECl_3 (E = Al, Ga) in fluorobenzene solution. The subsequent reaction with P_4 results in the precipitation of analytically pure products. The intriguing NMR spectra and molecular structures of the obtained cationic $[RP_5Cl]^+$-cages are discussed. Furthermore, we present an investigation of the reactions of dichlorophosphanes and the Lewis acid $GaCl_3$ in various stoichiometries which provides a deeper understanding of the species that are involved in these reactions. To gain an in depth understanding about the underlying reaction mechanisms of the formal "insertion reaction" we carried out quantum chemical calculations.

RESULTS AND DISCUSSION

The reactions of monochlorophosphanes R_2PCl and Lewis acids ECl_3 (E = Al, Ga) in organic solvents have been previously investigated.[8] The expected Lewis acid–base complexes **10** were observed in these reaction mixtures, but other compounds were also detected.[8] These include homoatomic coordination complexes of phosphenium cations, that is, phosphanylphosphonium salts $\mathbf{11}^+$ featuring P–P bonds,[9] and unstabilized cations $[R_2P]^+$ ($\mathbf{9}^+$).[10,2] Two-coordinate phosphenium cations $\mathbf{9}^+$ are main group carbene analogues that feature six valence electrons on the central atom.[11] Because of their inherent electrophilicity, most of the phosphenium ions are highly reactive and transient species. This hampers their direct observation in solution. However, structural characterization is possible in solution[12] and solid state[13] when the phosphenium cation is stablized by delocalization of the positive charge. The reactions of dichlorophosphanes $RPCl_2$ (**13**) and Lewis acids ECl_3 (E = Al, Ga) in organic solvents have been studied to a much lesser extent. The formation of Lewis acid–base complexes $m RPCl_2 \cdot n ECl_3$ (E = Al, m = 1, 2; n = 1, 2)[14] has been suggested, although the Lewis basicity of dichlorophosphanes is much lower in comparison to the corresponding monochlorophosphanes.[15] Such adducts were used for the in situ formation of phosphenium cations $[RPCl][AlCl_4]$ and the subsequent synthesis of phosphorus heterocycles.[16] Mixtures of mono- and dichlorophosphanes in the presence of Lewis acids result in the formation of chlorophosphanylchlorophosphonium cations $\mathbf{15}^+$, which were spectroscopically characterized by ^{31}P NMR for a variety of different substituents. In most cases, the spectra are sufficiently resolved at room temperature to detect the $^1J_{PP}$ coupling in the chlorophosphanylchlorophosphonium cations $\mathbf{15}^+$.[17] However, mixtures of dichlorophosphanes and a Lewis acid in CH_2Cl_2 show broad peaks in the ^{31}P NMR spectra. This indicates dynamic dissociation of the coordinated P–P bonds of the corresponding chlorophosphanyldichlorophosphonium cations $\mathbf{16}^+$ because of the weak donor abilities of dichlorophosphanes.[17]

^{31}P NMR Investigation of $RPCl_2/GaCl_3$ Mixtures. We have now performed a systematic investigation of the reaction of dichlorophosphanes $RPCl_2$, **13a–g** (a: R = *t*Bu, b: Cy, c: *i*Pr, d: Et, e: Me, f: Ph, g: C_6F_5) and ECl_3 (E = Al, Ga) in fluorobenzene, which we use as solvent in this study because of its beneficial properties during the synthesis of our phosphorus cages (vide infra). Our results show that, depending on the ratio of the reactants and the organic group on $RPCl_2$, mixtures of different neutral and cationic compounds are formed which in some cases show dynamic exchange. We start our discussion with the influence of various stoichiometries on the composition. The $^{31}P\{^1H\}$ NMR spectra of reaction mixtures of the dichlorophosphanes **13a–g** and $GaCl_3$ in fluorobenzene depend strongly on the ratio of the reactants. Table 1 summarizes the chemical shifts and coupling constants for the observed species in solution[18] for the stoichiometries 2:1, 1:1, 1:2, and 1:3 of dichlorophosphanes **13a–g** and $GaCl_3$ at room temperature.[19] Depending on the substituent R and the reaction stoichiometry, the formation of several structurally distinct species as well as some decomposition products as a result of solvent activation are observed (Chart 3). Figure 1 displays the $^{31}P\{^1H\}$ NMR spectra of the reaction mixtures of the selected dichlorophosphanes **13a,b,f** and $GaCl_3$ in the mentioned stoichiometries. Similar to previous studies,[17] the classical 1:1 complexes $RCl_2P–GaCl_3$ (**14**) are observed in reaction mixtures involving alkyl substituted dichlorophosphanes with reaction stoichiometries of $RPCl_2$ (**13a–e**) and $GaCl_3$ in the range from 1:1 to 1:3. A second possibility of adduct formation is described by the coordination of the gallium atom to one of the chlorine substituents of $RPCl_2$ forming compound $RClP–Cl–GaCl_3$ (**14′**). Similar species have been described as phosphenium ion equivalents within the system Ag^+/PX_3 fomally delivering a PX_2^+ cation.[20] However, we found that adduct **14a** is favored by $\Delta G_{298.15\,K}$ = 10.9 kcal/mol compared to adduct **14a′** according to quantum chemical calculations (MP2/TZVP, see Supporting Information for details). Thus, complex **14a** is essentially the only product in the 1:1 reaction mixture of **13a** and $GaCl_3$. The Lewis acid–base adducts **14a-e** show a consistent upfield shift of their ^{31}P NMR signals by approximately 60 ppm to higher field with respect to the free phosphanes **13a–e**. Similar high-field shifts were reported for the structurally related monochlorophosphane adducts **10**.[21] We were able to isolate and structurally characterize compound **14a** (Figure 2) from the 1:1 reaction of *t*BuPCl$_2$ with 1 equiv of $GaCl_3$ in fluorobenzene. Diffusion of *n*-hexane into the reaction mixture at −35 °C yielded small amounts of adduct **14a** as an extremely air and moisture sensitive, crystalline material that starts to melt above −25 °C. Compound **14a** crystallizes in the monoclinic space group $P2_1/n$ with four formula units in the unit cell. The compound represents the first structurally characterized Lewis acid-base adduct of $GaCl_3$ and a dichlorophosphane. The P–Ga bond

Chart 3. Potential Products from the Reaction of Chlorophosphanes and Lewis Acids ECl_3 (E = Al, Ga)[a]

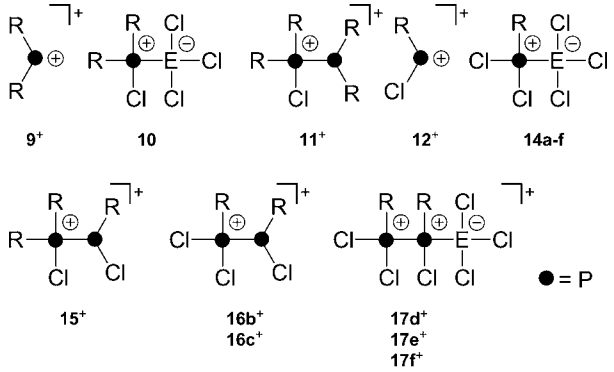

R = a: *t*Bu, b: Cy, c: *i*-Pr, d: Et, e: Me, f: Ph, g: C_6F_5

[a]Anions are not displayed.

dx.doi.org/10.1021/ic2013304 | Inorg. Chem. 2012, 51, 3374–3387

Table 1. ^{31}P NMR Data and Signal Assignments in Mixtures of Dichlorophosphanes (13a−g) and $GaCl_3$ in Fluorobenzene[a]

R	stoichiometry $RPCl_2$:$GaCl_3$	$RPCl_2$−$GaCl_3$ (**14**)	$[RPCl_2-PRCl]^+$ (**16**$^+$)	$[RPCl_2-PRCl-GaCl_3]^+$ (**17**$^+$)	$[RPCl_2H]^+$ (**18**$^+$)	$[RAr^FPCl-PRCl]^{+c}$ (**19**$^+$)	$[RAr^FPClH]^{+d}$ (**20**)	$RPCl_2$[e] (**13a-g**)
*t*Bu	2: 1	165 (14)						199
	1: 1	141 (20)						
	1: 2	139 (22)			99 [630]			
	1: 3	139 (20)			99 [630]		68 [550]	
Cy	2: 1	163 (97)	102 (140)					198
	1: 1	130 (35)	134, 99 [~490]		89 [650]			
	1: 2	129 (35)	134, 99 [498]		89 [645]		57 [550]	
	1: 3	128 (35)	134, 99 [498]		89 [645]		57 [550]	
*i*Pr	2: 1	170 (55)	105 (205)					200
	1: 1	165 (77)	101 (110)					
	1: 2	135 (25)	141, 104 [503]		95 [650]		62 [560]	
	1: 3	134 (19)	141, 104 [503]		95 [650]	99, 85 [420]; 93, 80 [420]	62 [560]	
Et	2: 1			138 (45), 104 (280)				196
	1: 1			133 (131), 100 (85)				
	1: 2	132 (172)		136, 100 [~420][b]	91 [670]	92, 79 [390]	55 [570]	
	1: 3	131 (71)		136, 100 [~460][b]	91 [670]	92, 79 [390]	55 [570]	
Me	2: 1			157 (67), 98 (106)				192
	1: 1			130 (40), 97 (46)				
	1: 2	127 (157)		130 (420), 97 (420)	85 [695]	83, 73 [370]; 83, 75 [368]	47 [570]	
	1: 3	127 (130)		130, 97 [~400][b]	85 [695]	83, 73 [370]; 83, 75 [369]	47 [570]	
Ph	2: 1			139 (87), 85 (99)				163
	1: 1			111 (35), 85 (31)				
	1: 2			110 (425), 85 (410)	69 [695]	70, 58 [393]; 71, 58 [395]		
	1: 3			110, 85 [~430][b]	69 [695]	70, 57 [395]; 70, 58 [397]		
C_6F_5	2: 1						22 [620]	135
	1: 1						22 [620]	
	1: 2						22 [620]	
	1: 3						22 [620]	

[a] $^{31}P\{^1H\}/^{31}P$ NMR-Data are given as chemical shifts are reported in ppm $^1J_{PP}$ values [in parentheses] and half widths (in brackets) in Hz. [b] Very broad resonances. [c] Two sets of AX spin systems are observed, resulting from Ar^F = o,p-C_6H_4F. [d] Only small amounts observed. [e] Chemical shift of the respective dichlorophosphane (**13a−g**) in fluorobenzene.

length [Ga1−P1 2.4252(9) Å] in **14a** is typical for phosphane-gallane complexes [2.35−2.68 Å][22] and comparable to those of related complexes such as $Cl_3Ga-Ph_2PPPh_2-GaCl_3$ [2.4285(6) Å].[4] Moreover, the phosphorus atom in **14a** shows a distorted tetrahedral environment [Ga1−P1−C1 121.2(1)°] because of the presence of the sterically demanding *t*Bu group, which adopts a staggered conformation with the $GaCl_3$ moiety.

It is noteworthy that, while the 1:1 to 1:3 mixtures of $RPCl_2$ (**13a-f**) and $GaCl_3$ gave distinct species in the ^{31}P NMR spectra, the 2:1 reactions showed broad signals (Figure 1). Thus, the 2:1 reaction mixture of **13a** and $GaCl_3$ gave rise to a broadened resonance at 165 ppm with a line width of $\nu_{1/2}$ = 14 Hz. We attribute the observed line broadening to a fast exchange process in solution (eq 1) between **13a** (δ = 199 ppm) and **14a** (δ = 141 ppm).

$$\underset{\mathbf{14}}{RPCl_2-GaCl_3} + \underset{\mathbf{13}}{RPCl_2} \rightleftharpoons \underset{\mathbf{13}}{RPCl_2} + \underset{\mathbf{14}}{RPCl_2-GaCl_3} \quad \text{(eq 1)}$$

Reducing the steric bulk and the basicity of the used dichlorophosphanes from *t*Bu (**13a**) to methyl (**13e**) results in significant changes in the $^{31}P\{^1H\}$ NMR spectra of the respective reaction mixtures (Table 1). Figure 1 (middle) displays the ^{31}P NMR spectra of solutions which contained $CyPCl_2$ (**13b**) and $GaCl_3$ in 2:1, 1:1, 1:2 and 1:3 ratios. As observed for the 2:1 mixture of **13a** and $GaCl_3$, the 2:1 reaction mixture of **13b** and $GaCl_3$ shows a broad resonance (δ = 163 ppm, $\nu_{1/2}$ = 97 Hz) as the main species. However, an additional broad signal (δ = 102 ppm, $\nu_{1/2}$ = 140 Hz) with low intensity indicates a second dynamic process. We believe that this observation may be attributed to the very fast and reversible reaction of **14b** and [RPCl][$GaCl_4$] to form species **16b**$^+$ (eq 2). Compounds of type **14** and **16**$^+$ have previously been proposed as structural alternatives that form equilibria in solution, and their relative stabilities depend upon the nature of the substituent (R) as well as reaction stoichiometry.[21]

$$\underset{\mathbf{14}}{RPCl_2-GaCl_3} + \underset{[\mathbf{12}][GaCl_4]}{[RPCl][GaCl_4]} \rightleftharpoons \underset{[\mathbf{16}][GaCl_4]}{[RPCl_2-RPCl][GaCl_4]} + GaCl_3 \quad \text{(eq 2)}$$

$$\underset{\mathbf{13}}{RPCl_2} + GaCl_3 \rightleftharpoons \underset{[\mathbf{12}][GaCl_4]}{[RPCl][GaCl_4]} \quad \text{(eq 3)}$$

Phosphanylphosphonium salts **16**$^+$ may be generated by the in situ formation of Lewis acidic phosphenium cations (**12**$^+$; eq 3) and subsequent coordination of a dichlorophosphane ligand according to eq 2.[2] This process is repressed by the equilibrium dissociation of $[GaCl_4]^-$ to yield chloride as well as the excess of

dx.doi.org/10.1021/ic2013304 | Inorg. Chem. 2012, 51, 3374−3387

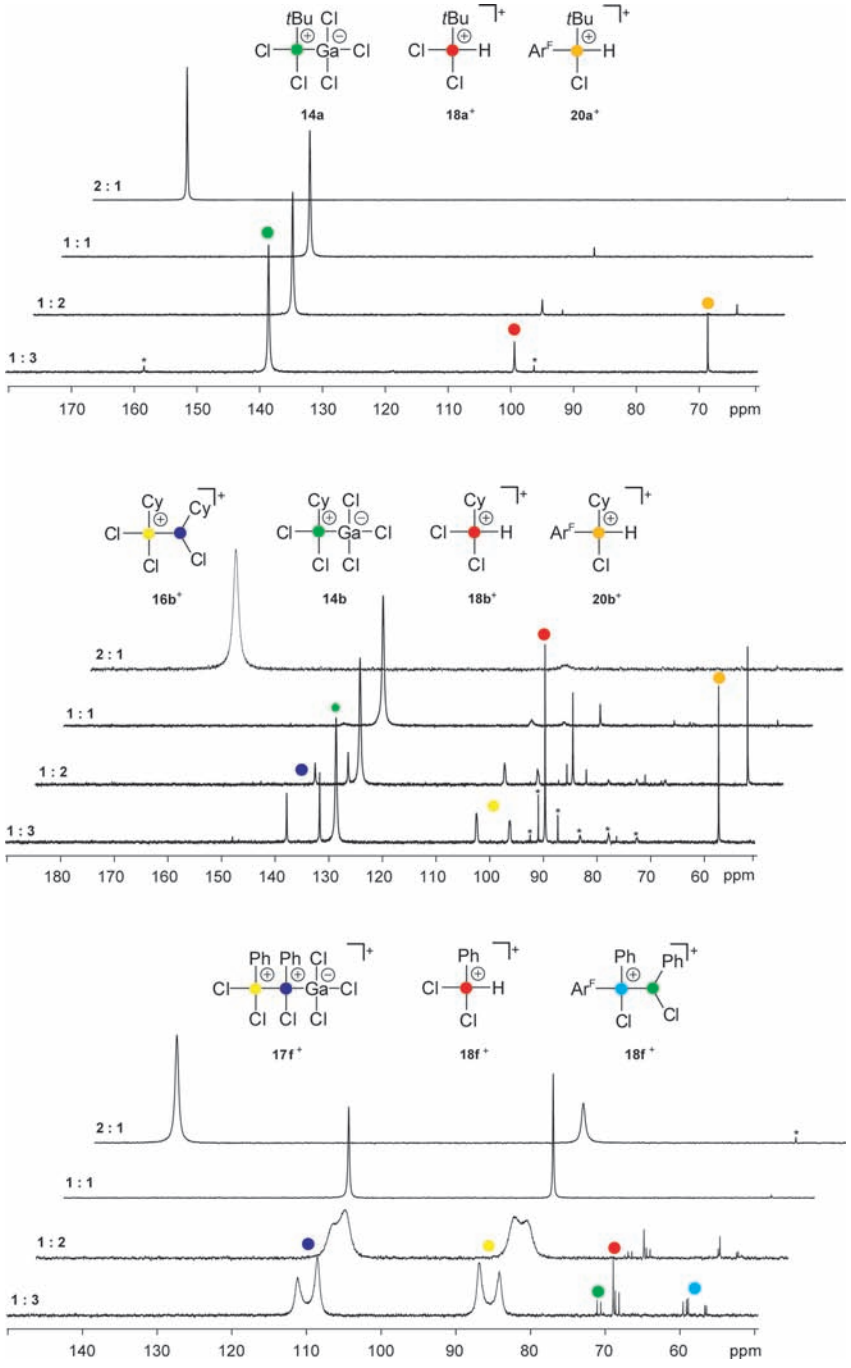

Figure 1. $^{31}P\{^{1}H\}$ NMR spectra (in fluorobenzene solution, C_6D_6-capillary, 27 °C, 81.01 MHz) of reaction mixtures of $RPCl_2$ and $GaCl_3$ in various stoichiometries; top: R = *t*Bu; middle: R = Cy; bottom: R = Ph. Small amounts of side products are indicated by an asterisk.

dichlorophosphanes which we propose undergo nucleophilic substitution reactions that lead to the dissociation of the formed complexes. The appearance of only one broad resonance for **16b**$^+$ again emphasizes this fast exchange process.[23] The addition of excess $GaCl_3$ suppresses nucleophiles, therefore, the 1:1 reaction mixture of $CyPCl_2$ and $GaCl_3$ shows, as a minor component, the two doublets (AB spin system, δ_A = 99, δ_B = 134 ppm; $^1J_{PP}$ = 490 Hz) that are typical for phosphanlyphosphonium cations. The donor–acceptor complex **14b** remains the main species in the reactions mixtures of $CyPCl_2$ and $GaCl_3$. However, this situation changes drastically when the basicity and steric requirements of the dichlorophosphanes are further reduced. Reaction mixtures of the less bulky $EtPCl_2$ and $MePCl_2$ with $GaCl_3$ exhibit the phosphanlyphosphonium complexes **17d,e**$^+$ as main products, and the donor–acceptor complexes **14d,e** are now the minor species. Cations **17d,e**$^+$ are probably formed from **14d,e** and **12**$^+$ according to eq 4. They were identified by two doublets in the $^{31}P\{^{1}H\}$ NMR spectra that are significantly broadened because of the influence of the quadrupole moment of the attached gallium atom as well as fast exchange processes.[21]

$$\underset{\mathbf{14}}{RPCl_2{-}GaCl_3} + \underset{[\mathbf{12}][GaCl_4]}{[RPCl][GaCl_4]} \rightleftharpoons \underset{[\mathbf{17}][GaCl_4]}{[RPCl_2{-}RPCl{-}GaCl_3][GaCl_4]} \quad \text{(eq 4)}$$

Similar to Cy and *t*Bu derivatives **13a** and **13b**, the ^{31}P NMR spectra of the 2:1 mixtures of **13d**, **13e**, and **13f** and $GaCl_3$

dx.doi.org/10.1021/ic2013304 | *Inorg. Chem.* 2012, 51, 3374–3387

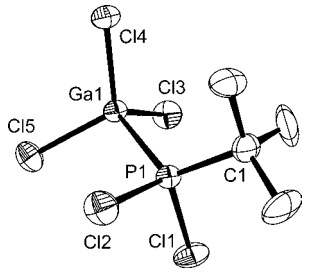

Figure 2. ORTEP plot of the molecular structure of **14a**. Thermal ellipsoids at 50% probability (hydrogen atoms are omitted for clarity). Selected bond lengths (Å) and angles (°): P1−C1 1.828(4), P1−Cl1 1.999(1), P1−Cl2 1.995(1), Ga1−P1 2.4252(9); C1−P1−Cl2 106.7(2), C1−P1−Cl1 106.6(1), Cl2−P1−Cl1 105.21(6), C1−P1−Ga1 121.2(1), Cl2−P1−Ga1 109.22(5), Cl1−P1−Ga1 106.83(5).

display two broad singlet resonances that result from the already discussed equilibria 1 and 4 in solution (eq 1 and 4). However, in the 1:1, 1:2, and 1:3 mixtures of **13f** and $GaCl_3$, the related adduct **14f** is not observed in the $^{31}P\{^1H\}$ NMR spectra (Figure 1, bottom). In this case equilibrium 4 (eq 4) dominates the reaction, and the main observed species is **17f**$^+$. The observed trend in the $^1J_{PP}$ couplings in derivatives **16**$^+$ and **17**$^+$ (Table 1) is explained by the σ-donor strength of the dichlorophosphanes,[24] which is influenced by inductive as well as steric effects of the substituent (for both criteria: Ph < Me < Et < *i*Pr < Cy <*t*Bu).[25] No reaction was observed in the $^{31}P\{^1H\}$ NMR spectra between dichlorophosphane **13g** (R = C_6F_5) possessing a very low basicity and $GaCl_3$. Phosphonium cations $[RPCl_2H]^+$ (**18a**−**g**$^+$) are observed in all reactions of dichlorophosphanes and $GaCl_3$ were the ratio is at least 1:1 (R = Cy) or an excess of $GaCl_3$ is used (R = *t*Bu, *i*Pr, Et, Me, Ph) (Table 1). The proton-coupled ^{31}P NMR spectra of these mixtures show an additional splitting of the corresponding resonance as a consequence of the one-bond coupling ($^1J_{PH}$ ranges from 620−695 Hz) of the hydrogen atom to the phosphorus atom in derivatives of **18**$^+$. They presumably originate in the reaction mixtures with an excess of $GaCl_3$ by direct Friedel−Crafts type arylation reactions of the dichlorophosphanes $RPCl_2$. This results in the formation of chlorophosphanes RAr^FPCl and one equivalent HCl. Because of the higher Lewis basicity of chlorophosphanes compared to dichlorophosphanes they are mainly observed in the reaction mixtures as $[RAr^FPClH]^+$ (**20a**−**g**$^+$, Ar^F = o,p-C_6H_4F).[26,27] Furthermore the formation of the corresponding phosphanylphosphonium salts $[RAr^FPCl{-}PRCl]^+$ (**19c**−**f**$^+$) are observed for less σ-donating organic substituents R. The latter species result from the reaction of $RPCl_2$ and $GaCl_3$ with RAr^FPCl and are mainly observed in the 1:2 and 1:3 reaction mixtures. The amount of **18**$^+$, **19**$^+$, and **20**$^+$ increases drastically with prolonged reaction times. In the case of **13g** the only side-product observed for all reactions stoichiometries is cation $[(C_6F_5)Ar^FPClH]^+$ (**20g**$^+$). The observed amount of this product significantly increases in reaction mixtures with an excess of $GaCl_3$ (Table 1).[28]

Raman Spectra of Selected $RPCl_2/GaCl_3$ Mixtures. Our findings are further supported by Raman spectroscopy. The Raman spectra of various reaction stoichiometries of $tBuPCl_2$ (**13a**) and $PhPCl_2$ (**13f**) with $GaCl_3$ in fluorobenzene are depicted in Figure 3. In both cases, characteristic bands of the free dichlorophosphanes **13a,f** are observed in the Raman spectra of the 2:1 mixtures (Table 2). This is in accord with the

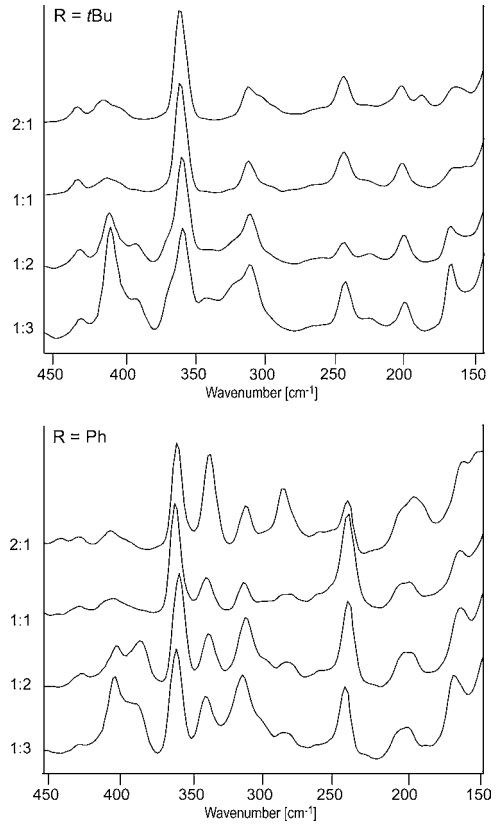

Figure 3. Raman spectra below 450 cm^{-1} of the reaction mixtures of $RPCl_2$ and $GaCl_3$ in various stoichiometries in fluorobenzene.

suggested equilibrium between adducts **14a,f** and the corresponding dichlorophosphanes (eq 1). Furthermore, all spectra display a series of modes that are associated with $Cl_3Ga{-}P$ vibrations [R = *t*Bu: 434, 406, 310, 199, 160 cm^{-1}; R = Ph: 441, 405, 320, 207 cm^{-1}], and are therefore expected for adducts **14a,f** and phosphanylphosphonium complexes **17f**$^+$ (eq 4). In the Raman spectrum of the 2:1 mixture of $PhPCl_2$ and $GaCl_3$ the characteristic band at 346 cm^{-1}, corresponding to the A_1 vibration mode of the tetrahedral $[GaCl_4]^-$ species, is observed. This band significantly decreases in the 1:1, 1:2 and 1:3 spectra, while bands [399, 287 cm^{-1}] appear, which can be attributed to the $[Ga_2Cl_7]^-$ anion. The presence of the $[Ga_3Cl_{10}]^-$ anion can be assumed since there are significant broader bands observed in the 1:2 and 1:3 mixture at approximately 390 cm^{-1} and 265 cm^{-1}. In addition, $[GaCl_4]^-$ anions are still present for the mentioned 1:2 and 1:3 stoichiometries. On the basis of these results, we suggest the equilibrium outlined in eq 5.[29]

$$2\,[Ga_2Cl_7]^- \rightleftharpoons [Ga_3Cl_{10}]^- + [GaCl_4]^- \quad \text{(eq 5)}$$

In contrast to the case of $PhPCl_2$ (**13f**), no bands are observed in the Raman spectra of $tBuPCl_2$ (**13a**) and $GaCl_3$ which can be attributed to the presence of the gallate anions $[GaCl_4]^-$, $[Ga_2Cl_7]^-$, or $[Ga_3Cl_{10}]^-$. Furthermore, for mixtures containing either **13a** or **13f** around 400 cm^{-1} and 165 cm^{-1} are observed, which we attribute to Ga_2Cl_6. This assignment is supported by the fact that the intensity of these bands increases with the concentration of $GaCl_3$. All assignments are in agreement with experimental data from the literature and are summarized in Table 2.[4,29,30]

dx.doi.org/10.1021/ic2013304 | *Inorg. Chem.* 2012, 51, 3374−3387

Table 2. Comparison of Bands in the Raman Spectra of Reaction Mixtures from $RPCl_2$ Reaction Mixtures of $RPCl_2$ (R = *t*Bu, Ph) and $GaCl_3$ in Fluorobenzene at RT in Various Stoichiometries

R = *t*Bu[a]				R = Ph[a]				
2: 1	1: 1	1: 2	1: 3	2: 1	1: 1	1: 2	1: 3	assignment[b]
				455 (vw)				$RPCl_2$
434 (w)	434 (w)	434 (w)	434 (w)	441 (vw)	441 (vw)	441 (vw)	439 (vw)	$\nu_{asym}[GaCl_2]$, $\delta[P-GaCl_3]$[d]
415 (w)	415 (w)	415 (m)	415 (s)	418 (w)	417 (w)	414 (m)	413 (s)	Ga_2Cl_6, $\nu_1[A_g]$
						399 (m)	398 (m, sh)	$Ga_2Cl_7^-$, $\nu_{sym}[Ga(Cl_t)_3]$
406 (vw, sh)	406 (vw, sh)	396 (w, sh)	396 (m, sh)	405 (vw)	*c*	*c*	*c*	$\nu[P-Ga]$[d]
359 (vs)	359 (vs)	359 (vs)	359 (vs)	370 (vs)	370 (vs)	370 (vs)	369 (vs)	$\nu_{sym}[P-GaCl_3]$[d]
					c	*c*	*c*	$Ga_2Cl_7^-$, $\nu_{asym}[Ga(Cl_t)_3]$
				346 (vs)	345 (m)	344 (m)	344 (m)	$GaCl_4^-$, $\nu_1[A_1]$
		342 (m)	342 (m)					Ga_2Cl_6, $2\nu_3$
		322 (m, sh)	322 (m, sh)			*c*	*c*	Ga_2Cl_6, $\nu_2[A_g]$
310 (w)	310 (m)	310 (m)	310 (m)	320 (w)	320 (w)	320 (m)	320 (s)	$\delta[P-Ga]$[d]
297 (w, sh)				292 (m)				$RPCl_2$
					287 (w, br)	287 (w, br)	287 (w, br)	$Ga_2Cl_7^-$, $\delta[Ga-Cl_b-Ga]$
241 (s)	241 (s)	241 (s)	241 (s)	245 (s)	245 (s)	245 (s)	245 (s)	PhF (solvent)
199 (w)	199 (m)	199 (m)	199 (m)	207 (m, sh)	207 (m, br)	207 (m, br)	201 (m, br)	$\delta[P-Ga]$[d]
185 (vw)				197 (m, sh)				$RPCl_2$
160 (vw)	163 (vw)	164 (m)	166 (s)		162 (m)	163 (s)	165 (s)	Ga_2Cl_6, $\nu_3[A_g]$, $\nu_{sym}[Ga-P]$[d]

[a]Intensity and appearance of bands are indicated by the following abbreviations: s = strong, m = medium, w = weak, v = very, br = broad, sh = shoulder, *t* = terminal, b = bridging. [b]Assignments of bands for Ga_2Cl_6, $GaCl_4^-$, $Ga_2Cl_7^-$, and $Ga_nCl_{3n+1}^-$ (n = 1−3) are based on data from the Ga/$GaCl_3$ system from ref 29. [c]Not observed because of overlapping of bands. [d]Assignments of bands have been carried out with the help of calculated Raman spectra for adduct **14a** (see Supporting Information for further details).

Weaker bands may be below the detection limit or may not be observed because of overlapping bands. The situation is further complicated by the fact that bands due to gallium(III)-arene modes are expected to occur in the same spectral range. Nevertheless, we believe that our findings strongly suggest that the very basic *t*BuPCl$_2$ (**13a**) exclusively forms adduct **14a** with $GaCl_3$, whereas 1:1 mixtures of $PhPCl_2$ (**13f**) and $GaCl_3$ and mixtures of **13f** which contain an excess of $GaCl_3$ give the phosphanylphosphonium salt **17f**$^+$. A mixture of both types of products is observed for the other combinations of dichlorophosphane and $GaCl_3$ (**13b**−**e**), in which the ratios of the observed species in solution strongly depend on the steric bulk and basicity of the phosphane. An in-depth Raman spectroscopic and ^{31}P NMR spectroscopic investigation of mixtures of dichlorophosphanes and $AlCl_3$ is hampered by the low solubility of the latter in fluorobenzene. Binary systems of $RPCl_2/AlCl_3$ in fluorobenzene are nevertheless reactive sources for chlorophosphenium cation equivalents $[RPCl]^+$ (eq 3) and can be used for the generation of functionalized $[RP_5Cl]^+$-cages **21**$^+$ (vide infra).

Quantum Chemical Calculations. According to recent investigations,[20,31] the formation of P_5 cage compounds via free phosphenium ions seemed unlikely. However, attempts to calculate a feasible reaction mechanism from the adducts of $GaCl_3$ with $RPCl_2$ (R = *t*Bu, Me) as sources of phosphenium ions and P_4 to form P_5 cage cations were unsuccessful at the B3LYP/6-31G(d) and MP2/6-31G(d) levels of theory. Therefore, the reaction of P_4 with phosphanylphosphonium salt **16e**$[GaCl_4]$ as a source of a phosphenium ion was investigated at the B3LYP/6-31G(d) and subsequently refined at the MP2/6-31G(d) level of theory. A single step insertion of the phosphenium moiety into the P−P bond of the P_4 tetrahedron (Scheme 1) and a two step reaction path via butterfly type compound **22** (Scheme 2) were found to be viable.

Scheme 1. Reaction Pathway for the Formation of 21e$[GaCl_4]$ via a One Step Phosphane Assisted Phosphenium Ion Insertion

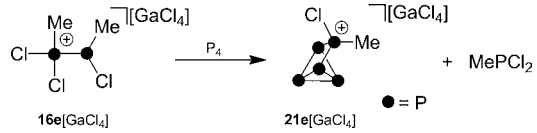

Scheme 2. Reaction Pathway for the Formation of 21e$[GaCl_4]$ via a Two Step Mechanism Including the Formation of Butterfly Type Intermediate 22

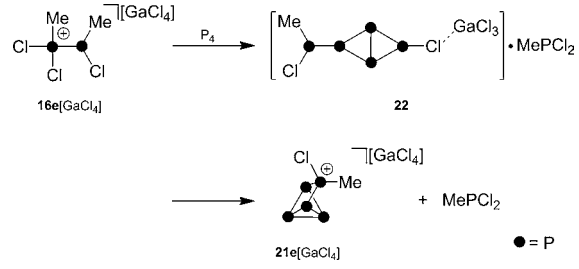

Figure 4 shows the calculated energy profile of both reaction paths. With a barrier of 21.1 kcal/mol (ΔH_{298}, TS1) a single step transfer of the phosphenium moiety in **16e**$[GaCl_4]$ and insertion thereof into a P−P bond of the P_4 tetrahedron is energetically viable (black path). In the light of recent mechanistic studies on the reaction of an isoelectronic silylene with P_4[32] this is best understood as a combined electrophilic and nucleophilic attack of the phosphenium moiety at P_4. On the one hand the P−P bond of P_4 (highest occupied molecular orbital, HOMO) nucleophilically attacks the p-type orbital of the phosphenium moiety. On the other hand the lone pair of electrons of the phosphenium moiety donates electron density into the lowest unoccupied molecular orbital (LUMO) of the P_4 tetrahedron which corresponds to p-orbitals situated

dx.doi.org/10.1021/ic2013304 | Inorg. Chem. 2012, 51, 3374−3387

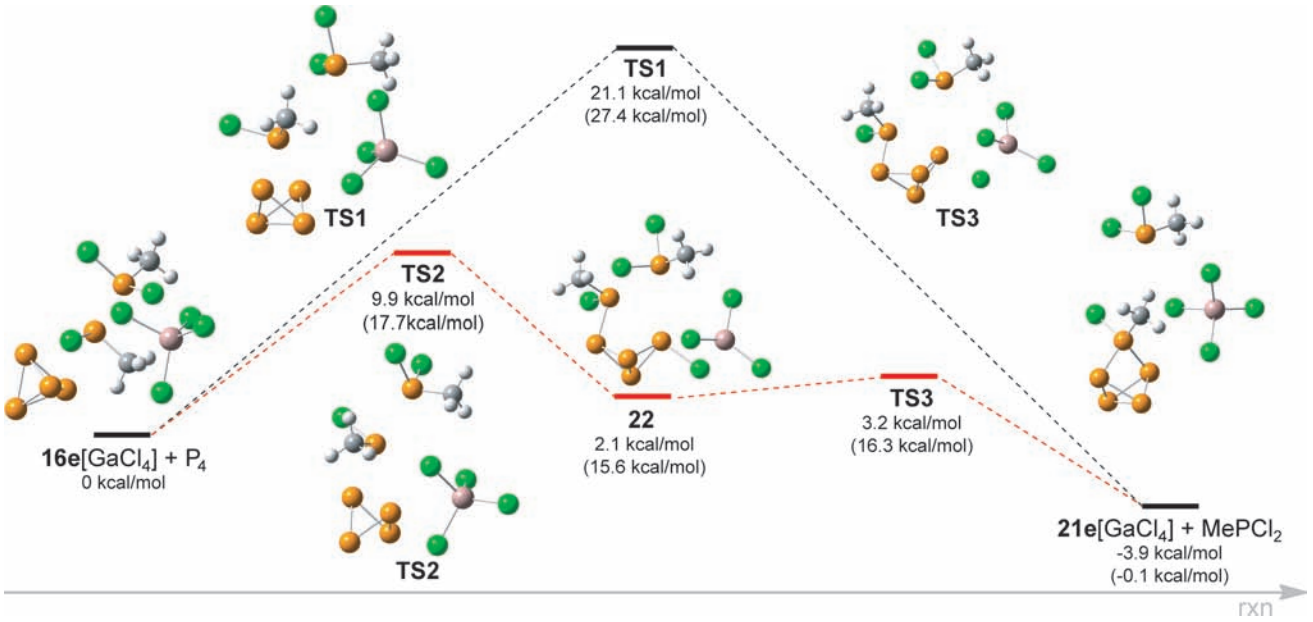

Figure 4. Calculated reaction pathways for the reaction of **16e**$[GaCl_4]$ and P_4. Calculated differences of the enthalpies at 298.15 K (ΔH_{298}) are given for the B3LYP/6-31G(d) and MP2/6-31G(d) (in parentheses) optimized structures. The optimized structures of **16e**$[GaCl_4]$ + P_4 were defined as 0 kcal/mol.

perpendicular to the P_4 lone pairs.[32] It was found however, that a lower barrier reaction path is accessible when the phosphenium cation does not act as a nucleophile. Instead a chlorine substituent of the tetrachlorogallate anion may nucleophilically attack the P_4 tetrahedron. Along with the electrophilic attack of the phosphenium moiety on P_4 this leads to the slightly endothermic formation of a butterfly type structure **22** (ΔH_{298} = 2.1 kcal/mol) via transition state TS2 ($\Delta H_{298\ K}$ = 9.9 kcal/mol, red path). Intermediate **22** can then rearrange via TS3 ($\Delta H_{298\ K}$ = 3.3 kcal/mol) to the P_5-cage compound **21e**$[GaCl_4]$ and $MePCl_2$. Calculations on the MP2/6-31G(d) level yielded related pathways with higher but still reasonable barriers (ΔH_{298} = 27.4 kcal/mol for TS1, 17.7 kcal/mol for TS2 and 16.3 kcal/mol for TS3). It is therefore most likely that the formation of the cationic P_5-cage compounds proceeds via a two-step reaction with structures of type **22** as intermediates and may be best described as an adduct formation, addition, and subsequent rearrangement reaction.

Syntheses and Characterization of the P_5 Cage Compounds [21a−g][ECl_4]. Dissolution of recrystallized P_4 in 1:1 mixtures of dichlorophosphanes **13a−f** and ECl_3 (E = Al, Ga) in fluorobenzene yielded white to yellowish precipitates of **21a−g**$[ECl_4]$ (Scheme 3). After workup, which included

Scheme 3. Preparation of Compounds 21a−g$[ECl_4]$ from P_4, $RPCl_2$, and ECl_3 in Fluorobenzene at RT (E = Al, Ga)

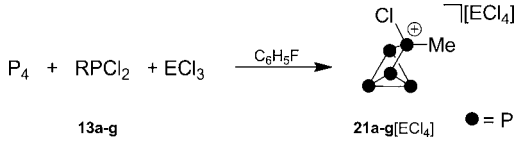

filtration and washing with *n*-hexane or recrystallization from dichloromethane, the salts **21a−g**$[ECl_4]$ are obtained as analytically pure compounds (>97% purity) in good to excellent yields (Table 3). Trace impurities of white phosphorus can be removed by vacuum sublimation at room temperature. In general, highly pure compounds **21a−g**$[ECl_4]$ show low solubilities in 1,2-difluorobenzene, fluorobenzene, and dichloromethane. However, addition of small amounts (<5 mol-%) of Lewis acid ECl_3 (E = Al, Ga) increases their solubilities drastically.[33] Compounds **21a−g**$[ECl_4]$ are air, moisture, and slightly light-sensitive. They readily decompose in coordinating solvents such as MeCN.

The salts are stable in substance for at least six month when stored at low temperatures in the dark. The $^{31}P\{^1H\}$ NMR spectra of the dissolved salts in dichloromethane at room temperature are depicted in Figure 5. Iterative line shape fitting[36] of the observed spin systems yielded chemical shifts and coupling constants typical for C_s-symmetric P_5 cages with four chemically unequal phosphorus nuclei (Table 3). Because of the reduced symmetry of the $[RP_5Cl]^+$-cages compared to the C_{2v}-symmetric $[R_2P_5]^+$-cages,[3,5] ABM_2X spin systems are observed for cations **21a−d**$^+$ and $ABMX_2$ spins systems are detected for cations **21e−g**$^+$. Due to similar geometry of the P_5 core of cations **21a−g**$^+$, the $^1J_{PP}$ and $^2J_{PP}$ coupling constants deviate only marginally from each other (Table 3). However, the chemical shifts are strongly dependent on the substituent attached to the P_5 cages. The values of Taft's σ^* parameter[37] for the alkyl and aryl groups (Table 3) show an approximate linear correlation with the chemical shift of the respective phosphorus atom (Figure 6). The differences in chemical shifts are strongest for the tetra-coordinate phosphonium moieties (marked by a red dot, Figure 5), which show shifts ranging from 99 ppm (**21a**$^+$, R = *t*Bu) to 26 ppm (**21g**$^+$, R = C_6F_5). A reverse trend is observed for the resonances of the chemically equivalent bridging phosphorus atoms, which range from 44 to 83 ppm (marked by a blue dot, Figure 5). The tri-coordinate phosphorus atoms opposite the tetra-coordinate phosphorus atoms appear in a chemical shift range from −295 to −246 ppm (marked by yellow or green dots, Figure 5). It is not trivial to distinguish the two tricoordinate phosphorus atoms opposite the tetra-coordinate moiety, but the assignment of the resonances of each phosphorus nucleus in the cages **21a−g**$^+$

dx.doi.org/10.1021/ic2013304 | *Inorg. Chem.* 2012, 51, 3374−3387

Table 3. $^{31}P\{^1H\}$ NMR Parameters for $[RP_5Cl]^+$ Cations 21a–g$^+$[a], Taft's σ* Parameter for Alkyl and Aryl Groups, and Yields of 21a–g$[ECl_4]$ (E = Al, Ga)

	21a$^+$	21b$^+$	21c$^+$	21d$^+$	21e$^+$	21f$^+$	21g$^+$
spin system[b,c]	ABM_2X	ABM_2X	ABM_2X	ABM_2X	$ABMX_2$	$ABMX_2$	$ABMX_2$[g]
δ_A[d]	−295	−283	−283	−286	−287	−285	−284
δ_B	−278	−279	−281	−270	−260	−284	−246
δ_M	44	54	54	66	69	55	26
δ_X	99	85	89	80	81	76	83
$^1J_{AM}$; $^1J_{AX}$[d,e]	−140	−135	−135	−134	−134	−144	−137
$^1J_{BM}$; $^1J_{BX}$	−136	−141	−142	−142	−143	−133	−142
$^1J_{AB}$	−181	−180	−180	−177	−175	−179	−172
$^1J_{MX}$	−283	−280	−281	−279	−277	−281	−307
$^2J_{AM}$; $^2J_{AX}$	2	23	23	24	25	3	26
$^2J_{BM}$; $^2J_{BX}$	24	−2	0	0	3	23	10
R	*t*Bu	Cy	*i*Pr	Et	Me	Ph	C_6F_5
σ*[f]	−0.30	−0.26	−0.19	−0.10	−0.00	0.60	1.10
yield $[ECl_4]^-$ salts [%]	65	90	81	64	79	90	62
E = Ga, Al	77	94	74	80	85	94	67

[a] $^{31}P\{^1H\}$ NMR data of the $[GaCl_4]^-$ and $[AlCl_4]^-$ salts are similar (in CD_2Cl_2, 25 °C). [b] Designation of spin system by convention. Furthest downfield resonance is denoted by the latest letter in the alphabet, and furthest upfield by the earliest letter: $\Delta\delta(P_iP_{ii})/JP_iP_{ii} > 10$ (resonance considered to be pseudo first order and the assigned letters are separated) < 10 (consecutive letters are assigned). [c] All parameters were derived by iterative fitting of experimental at 161.94 MHz. [d] Chemical shifts (δ) are given in [ppm] and coupling constants (J) in [Hz]. [e] The absolute sign of the $^1J_{PP}$ have been tentatively assigned to be negative. [f] Tafts's σ* values for alkyl and aryl groups (R = *t*Bu, Cy, *i*Pr, Et, Me, Ph) taken from ref 34 and for R = C_6F_5 from ref 35. [g] Additional phosphorus-fluorine coupling has to be considered in the full line shape iteration: $^3J_{MF}$ = 5.8 Hz, $^4J_{XF}$ = 32.3 Hz, $^4J_{MF}$ = 4.7 Hz.

was achieved by a detailed analysis of the respective spin systems and the ^{31}P NMR coupling constants are presented in Table 3. According to Figure 7, the unsymmetrical substituted P_5 cage can be divided by a plane, spanned by the tetra-coordinate and bridging tricoordinate phosphorus atoms, into a $\mathbf{H}_{Cl}$- and $\mathbf{H}_R$-hemisphere. The $\mathbf{H}_{Cl}$-hemisphere contains the chloride substituent and the $\mathbf{H}_R$-hemisphere the alkyl or aryl substituents. The different types of $^1J_{PP}$ and $^2J_{PP}$ coupling constants in each cation are sufficiently different to allow for an unambiguous assignment of the chemical shift of each phosphorus atom by comparison. Although it is known that the $^1J_{PP}$ coupling constants can strongly depend on parameters such as oxidation state, coordination number, electronic effects of the substituents, and the presence or absence of localized electron pairs, we have assigned the absolute value of the $^1J_{PP}$ coupling to be negative in agreement with previous studies.[38] With the sign of $^1J_{PP}$ predetermined, the sign of the $^2J_{PP}$ coupling constants is obtained from the fit. Two sets of $^1J_{PP}$ and $^2J_{PP}$ coupling constants are observed between the tricoordinate phosphorus atoms (whose resonances are marked by blue, yellow, and green dots in Figure 5) and the tetra-coordinate phosphorus atoms (whose resonances are marked by a red dot in Figure 5). The nature of the substituents at the tetra-coordinate atom controls both the coupling constants $^{1,2}J_{PP}$ and to a considerable extent the chemical shifts. This is not only attributed to the electronic effects of the substituents (vide supra) but is also caused by "cross-ring through space" interaction of the lone pairs on the phosphorus atoms and the respective substituent.[39] Thus, the phosphorus signals marked in green are assigned to the $\mathbf{H}_{Cl}$-hemisphere since the respective chemical shifts are only slightly different and range from −278 to −287 ppm. The $^1J_{PP}$ and $^2J_{PP}$ couplings of these phosphorus atoms to the bridging and tetra-coordinate P atoms are close to ∼−135 Hz and ∼22 Hz, respectively. The signals marked in yellow are assigned to the $\mathbf{H}_R$-hemisphere. The respective chemical shifts strongly depend on R and range from −295 to −246 ppm (vide supra). For those nuclei, the $^1J_{PP}$ and $^2J_{PP}$ couplings to the bridging and tetra-coordinate phosphorus atoms are close to ∼−142 Hz and ∼2 Hz, respectively. Comparison of the $^2J_{PP}$ coupling constants with those observed in the symmetrically substituted R_2P_5-cations (R = Ph, $^2J_{PP}$ = 8 Hz;[5] R = Cl, Br, I, $^2J_{PP}$ = 26 Hz[3]) strongly supports our assignment according to Figures 5 and 8. The $^1J_{PP}$ coupling constants between the tetra-coordinate phosphorus atoms and the bridging phosphorus atoms show a larger value, typically found for phosphanylphosphonium cations,[40] and range from −277 to −307 Hz (Table 3).

The $^{31}P\{^1H\}$ NMR spectrum of the reaction mixture of **13g**, P_4 and $GaCl_3$ in fluorobenzene in a 1:1:1 ratio shows the $ABMX_2$ spin system of cation **21g**$^+$ (Figure 8). An interesting feature of this spectrum (fitted spectrum as insets in Figure 8) is the additional coupling to the *ortho*- and *meta*-fluoro substituents of the C_6F_5-group. The X_2 part of the spin system is, therefore, split into a doublet of triplett of triplett arising from the additional "through space" $^4J_{PF}$ enlarged coupling constant of 32 Hz.[41] The small additional splitting of the resonance for the tetra-coordinate phosphorus atom originates from the $^3J_{PF}$ coupling constant with a value of 6 Hz. This small value can be explained as due to cancellation of a positive "through space" contribution form the lone pair interaction of the bridging phosphorus atoms and the *ortho*-fluorine substituent and a negative "through bond" contribution. This "through space" coupling path is further supported by the X-ray analysis of the solid-state structure of **21g**$[GaCl_4]$.[42]

Compounds **21b–g**$[GaCl_4]$ have been crystallographically characterized, confirming their identities as the first examples of nonsymmetrically substituted cationic P_5-cages. Suitable crystals for X-ray investigations were obtained by diffusion of *n*-hexane into CH_2Cl_2 solutions of the respective salts. Table 4

dx.doi.org/10.1021/ic2013304 | Inorg. Chem. 2012, 51, 3374–3387

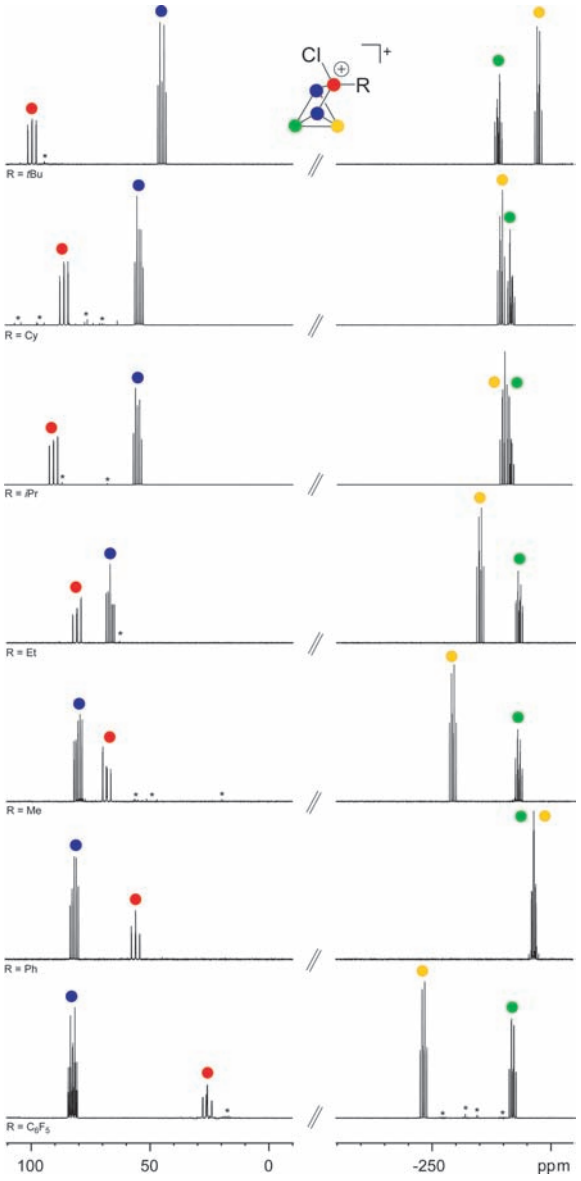

Figure 5. $^{31}P\{^{1}H\}$ NMR spectra of cations **21a**–**g**$^{+}$ (in CD_2Cl_2, 300 K, 161.94 MHz). Signals assigned to unknown side-products are labeled with asterisks.

lists selected structural parameters of the cages **21b**–**g**$^{+}$, and Figures 9 and 10 show ORTEP views of each cation. Crystallographic data and details of the structure refinement of compounds **21b**–**g**$[GaCl_4]$ are presented in Table 5. The P_5 cages in cations **21b**–**g**$^{+}$ display nearly identical bond lengths and angles. The P–P bond lengths in cations **21b**–**g**$^{+}$ (2.1511(9) to 2.258(2) Å) are very close to the values found in the symmetrically substituted $[P_5Br_2]^{+}$ (2.150(7) to 2.262(8) Å)[3] and $[Ph_2P_5]^{+}$ ion (2.179(1) to 2.249(1) Å).[5] Similar to the latter C_{2v}-symmetric cages, the bonds between the bridging (P2, P3) and tetra-coordinate phosphorus atoms (P1) and the P4–P5 bond in cations **21b**–**g**$^{+}$ are approximately 0.08 Å shorter (2.1511(9) to 2.1981(6) Å) than the remaining P–P bonds (2.257(1) to 2.232(1) Å). A short P4–P5 bond length has been observed for all reported cationic P_5-cages.[3,5-7] Similarly short P–P bond lengths were also detected in a related SiP_4 cage compound (2.159(2) Å)[43] and in bicyclo[1.1.0]-tetraphosphanes, R_2P_4 (R = organyl) which display relatively short P–P bridgehead

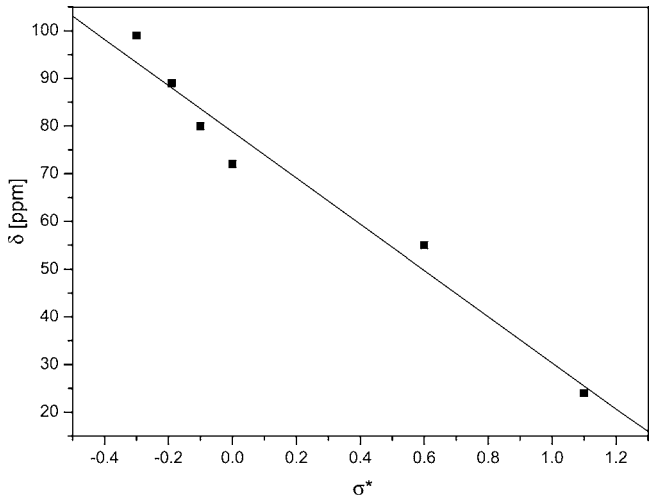

Figure 6. δ vs σ^* plot for the phosphonium nuclei in cations **21a,c**–**g**$^{+}$. The correlation coefficient is 0.9830.

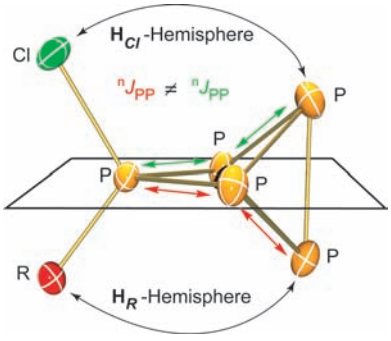

Figure 7. Definition of the $\mathbf{H}_{Cl}$- and $\mathbf{H}_{R}$-hemisphere in cages **21a**–**g**$^{+}$. The tetra-coordinate and bridging tricoordinate phosphorus atoms span a plane. The tricoordinate phosphorus atom above the plane lies within the $\mathbf{H}_{Cl}$-hemisphere (marked by green dots, Figure 5), the phosphors atom below in the $\mathbf{H}^{R}$-hemisphere (marked by a yellow dots, Figure 5).

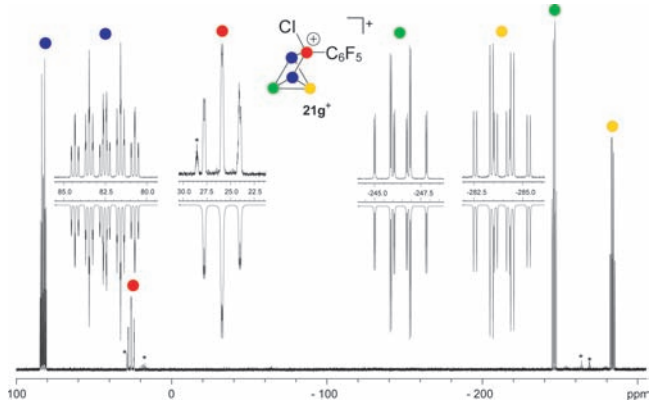

Figure 8. $^{31}P\{^{1}H\}$ NMR spectrum of cation **21g**$^{+}$ (C_6D_6-capillary, C_6H_5F, 25 °C, 161.94 Hz). Signals assigned to unknown side-products are labeled with asterisks. Expansion (inset) show the experimental (up) and fitted[36] (down) spectra of cation **21g**$^{+}$.

bonds (2.120 Å).[44] There are several examples of rather short P–P single bond distances involving cationic four-coordinate phosphorus atoms.[2,9,45,46] This shortening may be caused by the positive charge at the phosphonium moiety which also results in a

dx.doi.org/10.1021/ic2013304 | Inorg. Chem. 2012, 51, 3374–3387

Table 4. Selected Bond Length [Å] and Angles [°] of $[RP_5Cl]$-Cations 21b–g^{+a}

	21b$^+$	21c$^+$	21d$^+$	21e$^+$	21f$^+$	21g$^+$
P1–Cl1	2.013(2)	2.0093(9)	2.0167(5)	1.996(2)	2.0040(5)	2.0078(9)
P1–C1	1.809(4)	1.833(3)	1.799(2)	1.823(7)	1.786(2)	1.802(2)
P1–P2	2.156(2)	2.1597(9)	2.1630(6)	2.162(1)	2.1644(5)	2.1621(9)
P1–P3	2.163(2)	2.1594(9)	2.1559(5)	2.163(1)	2.1615(5)	2.1511(9)
P2–P4	2.258(2)	2.239(1)	2.2462(6)	2.245(1)	2.2496(6)	2.246(1)
P2–P5	2.241(2)	2.2546(9)	2.2406(6)	2.257(1)	2.2428(6)	2.232(1)
P3–P4	2.256(2)	2.2393(9)	2.2358(6)	2.250(1)	2.2491(6)	2.250(1)
P3–P5	2.243(2)	2.2541(9)	2.2501(6)	2.253(1)	2.2533(6)	2.252(1)
P4–P5	2.161(2)	2.170(1)	2.1851(6)	2.178(1)	2.1689(6)	2.185(1)
Cl1–P1–C1	104.4(1)	102.60(9)	105.39(5)	104.3(2)	107.58(5)	103.88(8)
P2–P1–P3	91.00	91.57(3)	91.54(2)	91.41(4)	90.68(2)	92.59(4)
P2–P1–C1	118.3(2)	115.91(9)	117.17(6)	119.3(4)	115.39(5)	114.96(8)
P3–P1–Cl1	111.69(6)	113.30(4)	110.61(2)	114.2(2)	112.94(2)	115.03(4)
P1–P2–P5	83.61(5)	81.08(3)	82.05(2)	82.17(4)	83.73(2)	83.89(4)
P1–P2–P4	84.58(6)	85.18(3)	83.86(2)	84.67(4)	84.60(2)	80.34(3)
P5–P2–P4	57.42(5)	60.75(3)	58.29(2)	57.87(4)	57.74(2)	58.41(3)
P4–P5–P2	61.71(5)	61.48(3)	60.99(2)	60.87(4)	61.29(2)	61.13(3)
P2–P5–P3	86.81(6)	86.72(3)	87.12(2)	86.68(4)	86.37(2)	88.14(4)
P5–P4–P3	60.98(5)	61.46(3)	61.18(2)	61.14(4)	61.30(2)	60.99(4)

^{a}All bond length and angles in the $[GaCl_4]^-$ anion show typical values.

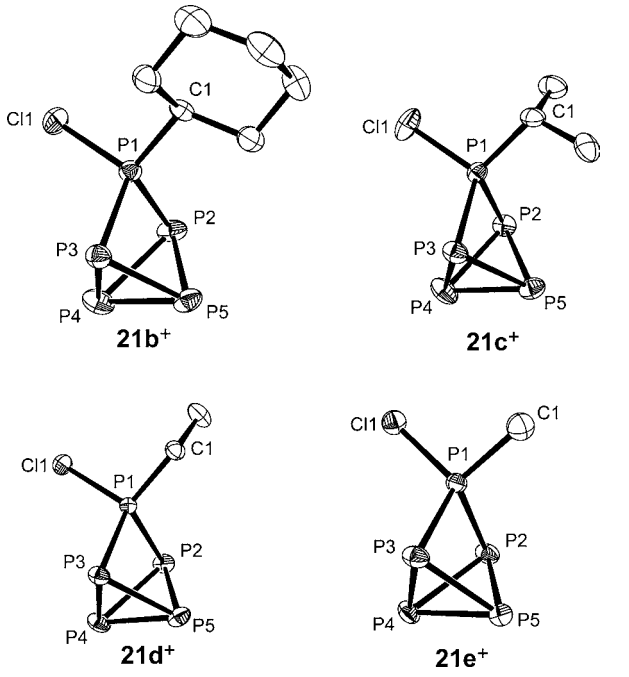

Figure 9. ORTEP representation of the molecular structures of the cations **21b–e**$^+$ in compounds **21b–e**$[GaCl_4]$. Thermal ellipsoids are set at 50% probability. Hydrogen atoms and anions are omitted for clarity.

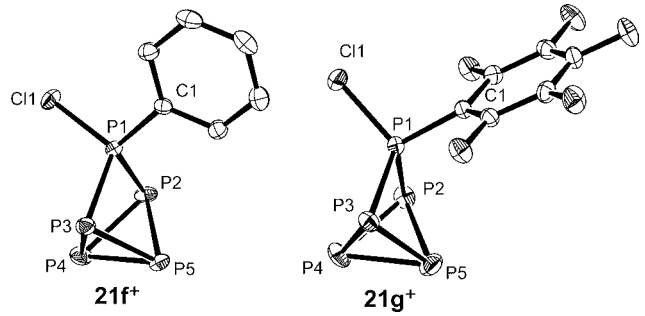

Figure 10. ORTEP representation of the molecular structures of the cations **21f,g**$^+$ in compounds **21f,g**$[GaCl_4]$. Thermal ellipsoids are set at 50% probability. Hydrogen atoms and anions are omitted for clarity.

significant shortening of the P–C (ranging from 1.786(2) to 1.833(3) Å) and P–Cl bonds (ranging from 1.996(2) to 2.0167(5) Å) compared to chloro- and alkyl- or aryl-substituted phosphanes (typical bond length for P–C: 1.87 Å and P–Cl: 2.04 Å).[47] A special feature in cation **21g**$^+$ is the observation of an intramolecular contact between the phosphorus atom P3 and one of the *ortho*-fluorine atoms of the C_6F_5-substituent (2.947(2) Å) which lies well within the sum of the van der Waals radii ($r_F + r_P$ = 3.27 Å).[48] This interaction is in agreement with the observed large $^4J_{PF}$ coupling constant in the $^{31}P\{^1H\}$ NMR spectrum (vide supra) and is evidence in favor of the proposed "through space" interaction.

CONCLUSION

The composition of mixtures of $RPCl_2$ and $GaCl_3$ in fluorobenzene strongly depends on the basicity of $RPCl_2$ (R = *t*Bu, Cy, *i*Pr, Et, Me, Ph, C_6F_5) and the reaction stoichiometry. $^{31}P\{^1H\}$ NMR and Raman experiments show the formation of several structurally distinct species, including $RPCl_2 \cdot GaCl_3$ adducts, (**14**) and dichlorophosphanylchloro-phosphonium cations $[RPCl_2–RPCl]^+$ (**16**$^+$) and $[RPCl_2–RPCl–GaCl_3]^+$ (**17**$^+$). Despite their different compositions 1:1 mixtures of $RPCl_2$ and a Lewis acid ECl_3 (E = Al, Ga) are potent sources of reactive chlorophosphenium cation $[RPCl]^+$ equivalents, which insert formally into P–P bonds of dissolved P_4. The formal insertion reaction has been investigated with quantum chemical calculations, and we suggest a two-stage reaction mechanism via a butterfly shaped intermediate. This synthetic approach represents a general method and a powerful strategy for the synthesis of new cationic chloro-substituted

dx.doi.org/10.1021/ic2013304 | Inorg. Chem. 2012, 51, 3374–3387

organophosphorus $[RP_5Cl]^+$ cages. The reactions proceed cleanly for a wide range of different substituents on the dichlorophosphane to new chloro substituted monocations **21a-g**$^+$ isolated in good to excellent yields. The detailed ^{31}P NMR investigation of these cations enabled a deeper understanding of the electronic and steric influences of the substituents on the ^{31}P NMR parameters. Furthermore, the simplicity and viability of this reaction bodes well for the development of larger cages using P_4 as a starting material. Because of the presence of chloro substituents such cages are amenable to a host of subsequent further transformations.

EXPERIMENTAL SECTION

General Considerations. All reactions were carried out either in a glovebox or using standard Schlenk techniques under an inert Ar atmosphere. Dry, oxygen-free solvents were employed. P_4 was dried with Me_3SiCl and recrystallized from CS_2 prior to use. Reagent grade $GaCl_3$ and $AlCl_3$ were used as received from commercial suppliers. $PhPCl_2$, iPrPCl$_2$, and MePCl$_2$ were purchased from Sigma-Aldrich and freshly distilled prior to use. CyPCl$_2$,[49] tBuPCl$_2$,[50] and $C_6F_5PCl_2$[51] were prepared according to literature procedures. All NMR measurements were performed at 300 K on a Bruker AVANCE III 400 or a Bruker AVANCE II 200 ($RPCl_2/GaCl_3$ mixtures) spectrometer, and spectra were referenced either to residual solvent (^{1}H, ^{13}C) or externally [^{19}F (CCl_3F); ^{31}P (H_3PO_4); ^{27}Al ($Al(NO_3)_3$); ^{71}Ga ($Ga(NO_3)_3$)]. CD_2Cl_2 was purchased form Sigma-Aldrich and dried over CaH_2, vacuum distilled prior to use, and stored over 4 Å molecular sieves in the glovebox. To obtain the ^{31}P{^{1}H} NMR data for reaction mixtures, a C_6D_6 capillary was inserted in the NMR tube. For compounds which give rise to higher order spin-systems in their ^{31}P{^{1}H} NMR spectra, the resolution-enhanced ^{31}P{^{1}H} spectra were transferred to the software program gNMR, version 5.0, by Cherwell Scientific.[36] The full line shape iteration procedure of gNMR was applied to obtain the best match of the calculated to the experimental spectra along with the assignment of all the peaks revealed in the resolution-enhanced spectra. The signs for the $^1J(^{31}P,^{31}P)$ coupling constants were set negative and all other signs obtained accordingly.[38] The connectivity of the phosphorus cage compounds **21a**−**g**$^+$ was additionally proven by the use of 2-dimensional ^{31}P{^{1}H}^{31}P{^{1}H}-COSY NMR experiments. Melting points were recorded on an electrothermal melting point apparatus in sealed capillaries under Argon atmosphere and are uncorrected. Infrared (IR) spectra were recorded using a Perkin-Elmer Spectrum One FT-IR instrument. Raman spectra were recorded on a Bruker Ram II spectrometer, with Nd:YAG-Laser (1064 nm, 10−200 mW) in sealed glass capillaries. The intensities are reported in percent relative to the most intense peak and are given in parentheses. Elemental analyses were performed on a Vario EL III CHNS elemental analyzer at the IAAC, University of Münster, Germany, except for **21g**[$GaCl_4$] and **21g**[$AlCl_4$] because of the high content of fluorine.

^{31}P{^{1}H} NMR Experiments of Dichlorophosphane/$GaCl_3$ Mixtures. A solution of the dichlorophosphane **13a-f** (0.5 mmol) and $GaCl_3$ (0.25/0.5/1.0/1.5 mmol) in C_6H_5F (2 mL) was stirred for 15 min at room temperature after which ^{31}P{^{1}H} NMR and Raman spectra were recorded immediately (Tables 1, 2).

Synthesis of 14a. A solution of tBuPCl$_2$ (159 mg, 1.0 mmol) and $GaCl_3$ (176 mg, 1.0 mmol) in C_6H_5F (5 mL) was stirred for 2 h at room temperature. Diffusion of n-hexane into the reaction mixture at −35 °C yields small amounts of adduct **14a** as crystalline material. **14a** is very temperature sensitive and isolation needs to be performed at low temperatures (−35 °C); **14a**: 18% (60 mg, 0,2 mmol); mp > −25 °C; ^{1}H NMR (CD_2Cl_2, 25 °C, [ppm]): δ = 1.52 (d, 9H, CH_3, $^3J_{HP}$ = 22.7 Hz); ^{13}C{^{1}H} NMR (CD_2Cl_2, 25 °C, [ppm]): δ = 24.1 (3C, d, CH_3, $^2J_{CP}$= 9.8 Hz), 44.0 (1C, d, $C(CH_3)_3$, $^1J_{CP}$= 12.7 Hz); ^{71}Ga{^{1}H} NMR (CD_2Cl_2, 25 °C, [ppm]): δ = 259 (s, $\nu_{1/2}$ = 4500 Hz); ^{31}P{^{1}H} NMR (CD_2Cl_2, 25 °C, [ppm]): δ = 142.4 (1P, s, $\nu_{1/2}$ = 37 Hz).

General Synthesis of Compounds 21a−g[ECl_4] (E = Ga, Al). A mixture of the dichlorophosphane (1.0 mmol), ECl_3 (1.0 mmol), and freshly recrystallized P_4 (1.0 mmol) in C_6H_5F (5 mL) was stirred at room temperature. P_4 dissolves completely accompanied by the formation of a colorless to yellowish precipitate. After addition of n-hexane (2 mL), the precipitate was collected, washed with n-hexane (3 × 2 mL), and dried in vacuo. Note, excess P_4 can be removed by sublimation to yield analytical pure product. Additional manipulations and reaction times are given for each compound seperately (vide infra).

21a[ECl_4]. The reaction mixture was stirred for 2 d. The formed precipitates (contains unreacted P_4) were removed by filtration. The addition of hexane (4 mL) to the filtrate afforded a colorless precipitate which was separated by filtration, washed with n-hexane (3 × 2 mL), and dried in vacuo to yield analytically pure **21a**[ECl_4]; **21a**[$GaCl_4$]: Yield: 65% (298 mg); mp 145 °C (decomp.); IR (KBr, 25 °C, cm^{-1}): 2967 (s), 2957 (m), 2925 (w), 1470 (vw), 1455 (vs), 1399 (vw), 1369 (s), 1309 (vw), 1239 (w), 1171 (s), 1012 (m), 939 (w), 791 (m), 619 (m), 586 (s), 573 (vw), 542 (w), 457 (w); Raman (150 mW, 25 °C, cm^{-1}): 2971 (4), 2944 (3) 2901 (10), 1460 (5), 1175 (3), 794 (5), 566 (6), 542 (100), 460 (50), 440 (27), 392 (41), 364 (34), 342 (25), 213 (23), 159 (39), 123 (21), 106 (6); ^{1}H NMR (CD_2Cl_2, 25 °C, [ppm]): δ = 1.58 (9H, d, Me, $^3J_{HP}$ = 23.7 Hz); ^{13}C{^{1}H} NMR (CD_2Cl_2, 25 °C, [ppm]): δ = 24.3 (3C, d, CH_3, $^2J_{CP}$ = 3.9 Hz), 50.2 (1C, s, C); ^{71}Ga{^{1}H} NMR (CD_2Cl_2, 25 °C, [ppm]): δ = 249 (s, $\nu_{1/2}$ = 158 Hz); elemental analysis for $C_4H_9Cl_5GaP_5$ (458.97): calcd. C: 10.5, H 2.0; found: C 10.3, H 2.1; **21a**[$AlCl_4$]: Yield: 77% (297 mg); mp 130 °C (decomp.); IR (KBr, 25 °C, cm^{-1}): 2968 (vs), 2933 (vw), 1457 (s), 1395 (w), 1370 (s), 1309 (vw), 1241 (w), 1171 (s), 1095 (vw), 998 (m), 939 (w), 875 (w), 834 (vw), 791 (s), 766 (w), 677 (vw), 619 (2), 587 (vw), 571 (m), 542 (w), 481 (vs), 437 (vw); Raman (150 mW, 25 °C, cm^{-1}): 2972 (4), 2944 (4), 2901 (13), 1460 (6), 1175 (4), 794 (5), 567 (6), 542 (100), 458 (36), 440 (26), 392 (37), 366 (12), 359 (47), 348 (13), 213 (23), 161 (37), 128 (5), 105 (18); ^{1}H NMR (CD_2Cl_2, 25 °C, [ppm]): δ = 1.57 (9H, d, Me, $^3J_{HP}$ = 23.8 Hz); ^{13}C{^{1}H} NMR (CD_2Cl_2, 25 °C, [ppm]): δ = 24.2 (3C, d, CH_3, $^2J_{CP}$ = 3.9 Hz), 50.2 (1C, s, C); ^{27}Al NMR (CD_2Cl_2, 25 °C, [ppm]): δ = 104 (s, $\nu_{1/2}$ = 133 Hz); elemental analysis for $C_4H_9Cl_5AlP_5$ (416.23): calcd. C: 11.5, H 2.2; found: C 11.3, H 2.4.

21b[$GaCl_4$]. 2 h reaction time; yield: 90% (437 mg); mp 46.3−48.1 °C; IR (KBr, 25 °C, cm^{-1}): 2941 (vs), 2919 (s), 2875 (m), 2853 (w), 1444 (vs), 1291 (w), 1266 (s), 1194 (vw), 1176 (w) 1110 (vw), 1040 (vw), 995 (m), 916 (w), 888 (m), 844 (w), 815 (s), 743 (m), 620 (w), 572 (vs), 458 (m), 421 (w); Raman (150 mW, 25 °C, cm^{-1}): 2950 (15), 2878 (6), 2853 (4) 1432 (5), 1293 (7), 1268 (6), 1024 (9), 846 (3), 817 (6), 573 (8), 556 (7), 544 (100), 460 (35), 442 (48), 423 (4), 391 (38), 357 (63), 343 (36), 289 (7), 225 (5), 213 (21), 192 (18), 176 (13), 151 (10), 125 (65); ^{1}H NMR (CD_2Cl_2, 25 °C, [ppm]): δ = 1.34 (1H, m, C4H$_{ax}$), 1.50 (2H, m, C2H$_{ax}$), 1.59 (2H, m, C3H$_{ax}$), 1.83 (2H, m, C4H$_{eq}$); 2.05 (2H, m, C3H$_{eq}$); 2.23 (1H, m, C2H$_{eq}$), 3.08 (1H, m, C1H$_{ax}$); ^{13}C{^{1}H}-NMR (CD_2Cl_2, 25 °C, [ppm]): δ = 25.0 (1C, d, C1, $^1J_{CP}$ = 2.0 Hz), 25.4 (2C, d, C2/C6, $^2J_{CP}$ = 4.9 Hz), 25.7 (2C, d, C3/C5, $^3J_{CP}$ = 4.5 Hz), 25.8 (1C, s, C4); ^{71}Ga{^{1}H} NMR (CD_2Cl_2, 25 °C, [ppm]): δ = 248 (s, $\nu_{1/2}$ = 1500 Hz); elemental analysis for $C_6H_{11}Cl_5GaP_5$ (485.01): calcd.: C 14.9, H 2.3, found: C 14.9, H 2.1; **21b**[$AlCl_4$]: 2 h reaction time; yield: 84% (372 mg); mp 46.9−49.5 °C; IR (KBr, 25 °C, cm^{-1}): 2940 (vs), 2920 (s), 2880 (m), 2854 (vw), 1444 (s), 1292 (w), 1265 (s), 1194 (w), 1176 (w), 1110 (vw), 1023 (vw), 995 (m), 916 (w), 888 (w), 844 (w), 815 (s), 743 (w), 675 (m), 619 (vw), 572 (w), 542 (w), 481 (s) 387 (w); Raman (150 mW, 25 °C, cm^{-1}): 2947 (21), 2880 (3), 2855 (10), 1447 (6), 1294 (6), 1268 (8), 1024 (9), 847 (4), 817 (7), 573 (8), 557 (5), 544 (100), 460 (34), 442 (47), 390 (41), 364 (68), 358 (7), 347 (8), 289 (7), 225 (5), 213 (21), 192 (23), 176 (14), 130 (35); ^{1}H NMR (CD_2Cl_2, 25 °C, [ppm]): δ = 1.35 (1H, m, C4H$_{ax}$), 1.51 (2H, m, C2H$_{ax}$), 1.58 (2H, m, C3H$_{ax}$), 1.83 (2H, m, C4H$_{eq}$), 2.05 (2H, m, C3H$_{eq}$), 2.24 (1H, m, C2H$_{eq}$), 3.09 (1H, m, C1H$_{ax}$); ^{13}C{^{1}H} NMR (CD_2Cl_2, 25 °C, [ppm]): δ = 25.0 (1C, d, C1, $^1J_{CP}$ = 2.6 Hz), 25.6 (2C, d, C2/C6), 25.7 (2C, s, C3/C5), 25.8 (1C, s, C4); ^{27}Al-NMR (CD_2Cl_2, 25 °C, [ppm]): δ = 104 (s, $\nu_{1/2}$ = 95 Hz); elemental analysis for $C_6H_{11}Cl_5AlP_5$ (442.27): calcd. C: 16.3, H 2.5; found: C 16.3, H 2.4.

21c[$GaCl_4$]. 2 h reaction time; yield: 81% (360 mg); mp 125.8−127.3 °C; IR (KBr, 25 °C, cm^{-1}): 2967 (m) 2915 (w) 2862 (vw), 1456 (m), 1385 (m), 1366 (w), 1233 (m), 1030 (w), 863 (vw), 651

dx.doi.org/10.1021/ic2013304 | Inorg. Chem. 2012, 51, 3374−3387

Table 5. Crystallographic Data and Details of the Structure Refinement of Compounds 14a and 21b−g[$GaCl_4$]

	14a	21b[$GaCl_4$]	21c[$GaCl_4$]	21d[$GaCl_4$]	21e[$GaCl_4$]	21f[$GaCl_4$]	21g[$GaCl_4$]
formula	$C_4H_9Cl_5GaP$	$C_6H_{11}Cl_5GaP_5$	$C_3H_7Cl_5GaP_5$	$C_2H_5Cl_5GaP_5$	$CH_3Cl_5GaP_5$	$C_6H_5Cl_5GaP_5$	$C_6Cl_5F_5GaP_5$
M_r [g mol^{-1}]	335.05	484.96	444.91	430.88	416.85	478.92	568.88
dimension [mm^3]	0.27 × 0.22 × 0.10	0.12 × 0.03 × 0.02	0.32 × 0.07 × 0.2	0.20 × 0.06 × 0.03	0.20 × 0.14 × 0.04	0.09 × 0.05 × 0.02	0.19 × 0.04 × 0.02
color, habit	colorless plate	colorless plate	colorless plate	colorless plate	colorless plate	colorless plate	colorless rod
crystal system	monoclinic	orthorhombic	monoclinic	monoclinic	orthorhombic	monoclinic	monoclinic
space group	$P2_1/n$	$Cmc2_1$	$P2_1/c$	$P2_1/n$	$P2_12_12_1$	$P2_1/c$	$P2_1$
a [Å]	12.0362(7)	23.2837(5)	14.3092(9)	12.6761(6)	6.3462(4)	8.4378(5)	6.8661(8)
b [Å]	8.6708(5)	13.2160(3)	21.778(1)	8.9880(4)	9.2206(6)	15.2665(9)	8.802(1)
c [Å]	13.2467(8)	16.7780(3)	9.5931(6)	13.2882(6)	22.395(1)	12.3411(7)	14.108(2)
α [deg]	90	90	90	90	90	90	90
β [deg]	116.435(1)	90	96.350(1)	112.951(1)	90	92.307(1)	95.396(2)
γ [deg]	90	90	90	90	90	90	90
V [Å^3]	1237.9(1)	5162.7(2)	2971.3(3)	1394.1(1)	1310.5 (1)	1588.4(2)	847.6(2)
Z	4	12	8	4	4	4	2
T [K]	153(1)	153(1)	153(1)	153(1)	153(1)	153(1)	153(2)
ρ_c [g cm^{-3}]	1.798	1.872	1.989	2.053	2.113	2.003	2.229
F(000)	656	2856	1728	832	800	928	544
$\lambda_{MoK\alpha}$ [Å]	0.71073	0.71073	0.71073	0.71073	0.71073	0.71073	0.71073
μ [mm^{-1}]	3.377	2.816	3.252	3.462	3.679	3.050	2.918
absorption correction	SADABS	SADABS	SADABS	SADABS	SADABS	SADABS	SADABS
reflections collected	12275	15069	29945	137999	13457	17396	9477
reflections unique	2961	6703	7091	3327	3129	4266	4525
R_{int}	0.0257	0.0442	0.0435	0.0238	0.0407	0.0252	0.0185
reflection obs. [$F > 3\sigma(F)$]	2584	5370	5786	3008	2865	3803	4325
residual density [e Å^{-3}]	2.527, −0.645	0.781, −0.592	0.600, −0.456	0.378, −0.311	0.519, −0.647	0.366, −0.310	0.423, −0.276
parameters	103	243	257	119	110	154	199
GOF	1.039	0.995	1.017	1.061	1.047	1.012	1.041
R_1 [$I > 3\sigma(I)$]	0.0388	0.0373	0.0284	0.0196	0.0265	0.0191	0.0253
wR_2 (all data)	0.1036	0.0717	0.0691	0.0496	0.0529	0.0424	0.0621
CCDC	826493	826494	826495	826496	826497	826498	826499

(s), 561 (vs), 540 (m), 452 (w), 412 (w); Raman (150 mW, 25 °C, cm^{-1}): 2967 (23), 2917 (28), 2862 (7), 1439 (5), 1388 (5), 1369 (4), 1238 (3), 1080 (3), 1033 (3), 865 (7), 654 (4), 578 (13), 563 (17), 542 (100), 452 (63), 414 (34), 390 (51), 358 (100), 345 (40), 237 (21), 206 (21), 153 (92), 123 (47); ^{1}H NMR (CD_2Cl_2, 25 °C, [ppm]): δ = 1.49 (6H, dd, CH_3, $^2J_{HP}$ = 26.0 Hz, $^3J_{HH}$ = 7.0 Hz), 3.35 (1H, sept., CH, $^3J_{HH}$ = 7.0 Hz); ^{13}C{^{1}H}-NMR (CD_2Cl_2, 25 °C, [ppm]): δ = 15.3 (2C, d, CH_3, $^2J_{CP}$ = 1.9 Hz), 45.0 (1C, m, CH); ^{71}Ga{^{1}H} NMR (CD_2Cl_2, 25 °C, [ppm]): δ = 248 (s, $\nu_{1/2}$ = 1900 Hz); elemental analysis for $C_3H_7Cl_5GaP_5$ (444.94): calcd. C: 8.1, H 1.6; found: C 8.4, H 1.6; **21c**[$AlCl_4$]: **2** h reaction time Yield: 74% (298 mg); mp 156.9−158.1 °C; IR (KBr, 25 °C, cm^{-1}): 2967 (m), 2916 (vw), 2862 (vw), 1456 (m), 1386 (w), 1366 (w), 1233 (m), 1031 (w), 863 (w), 663 (vw), 652 (m), 563 (s), 541 (m), 487 (vw), 470 (vs); Raman (150 mW, 25 °C, cm^{-1}) 2970 (20), 2917 (22), 2863 (7), 1464 (5), 1388 (4), 1368 (3), 1235 (4), 1079 (3), 1037 (4), 866 (5), 565 (11), 544 (100), 454 (40), 415 (23), 391 (32), 361 (61), 349 (8), 238 (14), 207 (11), 178 (4), 164 (48), 132 (16); ^{1}H NMR (CD_2Cl_2, 25 °C, [ppm]): δ = 1.52 (6H, dd, CH_3, $^2J_{HP}$ = 26.0 Hz, $^3J_{HH}$ = 7.0 Hz), 3.38 (1H, sept., CH, $^3J_{HH}$ = 7.1 Hz); ^{13}C{^{1}H} NMR (CD_2Cl_2, 25 °C, [ppm]): δ = 15.2 (2C, d, CH_3, $^2J_{CP}$ = 2.0 Hz), 45.0 (1C, m, CH); ^{27}Al NMR (CD_2Cl_2, 25 °C, [ppm]): δ = 103.5 (s, $\nu_{1/2}$ = 10 Hz); elemental analysis for $C_3H_7Cl_5AlP_5$ (402.20): calcd. C: 9.0, H 1.8; found: C 9.3, H 1.8.

***21d**[GaCl$_4$]*. 2 h reaction time; yield: 64% (276 mg); mp 100.6−101.8 °C; IR (KBr, 25 °C, cm^{-1}): 2942 (m), 2903 (m), 2864 (vw), 1441 (w), 1385 (m), 1243 (w), 1132 (vw), 1015 (w), 1001 (m), 742 (vs), 696 (m), 570 (s), 547 (w), 531 (vs), 435 (s); Raman (150 mW, 25 °C, cm^{-1}): 2973 (10), 2934 (27), 2910 (25), 2873 (6), 1398 (5), 544 (100), 473 (25), 448 (52), 394 (53), 376 (53), 361 (78), 348 (85), 224 (25), 153 (80), 116 (20); ^{1}H NMR (CD_2Cl_2, 25 °C, [ppm]): δ = 1.53 (3H, dt, CH_3, $^3J_{HP}$ = 27.4 Hz, $^3J_{HH}$ = 7.5 Hz), 3.10 (2H, dqu, CH_2, $^2J_{HP}$ = 15.0 Hz, $^3J_{HH}$ = 7.5 Hz); ^{13}C{^{1}H} NMR (CD_2Cl_2, 25 °C, [ppm]): δ = 7.0 (1C, d, CH_3, $^2J_{CP}$ = 5.9 Hz), 39.4 (1C, m, CH_2); ^{71}Ga{^{1}H} NMR (CD_2Cl_2, 25 °C, [ppm]): δ = 240 (s, $\nu_{1/2}$ = 7700 Hz); elemental analysis for $C_2H_5Cl_5GaP_5$ (430.92): calcd. C: 5.6, H 1.2; found: C 6.0, H 1.4; **21d**[$AlCl_4$]: 2 h reaction time; yield: 80% (311 mg); mp 143.3−144.2 °C; IR (KBr, 25 °C, cm^{-1}): 2943 (m), 2904 (m), 1441 (w), 1386 (m), 1242 (vs), 1153 (w), 1015 (w), 1001 (s), 743 (vs), 697 (m), 571 (s), 548 (w), 532 (w), 501 (w), 434 (vw); Raman (150 mW, 25 °C, cm^{-1}): 2976 (12), 2932 (10), 2905 (16), 2866 (5), 1388 (7), 570 (15), 548 (60), 530 (51), 438 (100), 395 (46), 363 (14), 356 (60), 242 (24), 210 (82), 179 (10), 127 (14); ^{1}H NMR (CD_2Cl_2, 25 °C, [ppm]): δ = 1.52 (3H, dt, CH_3, $^3J_{HP}$ = 27.5 Hz, $^3J_{HH}$ = 7.6 Hz), 3.12 (2H, dqu, CH_2, $^2J_{HP}$ = 15.2 Hz, $^3J_{HH}$ = 7.6 Hz); ^{13}C{^{1}H} NMR (CD_2Cl_2, 25 °C, [ppm]): δ = 7.0 (1C, d, CH_3, $^2J_{CP}$ = 5.9 Hz), 39.4 (1C, m, CH); ^{27}Al NMR (CD_2Cl_2, 25 °C, [ppm]): δ = 103.7 (s, $\nu_{1/2}$ = 69 Hz); elemental analysis for $C_2H_5Cl_5AlP_5$ (388.18): calcd. C: 6.2, H 1.3; found: C 6.7, H 1.5.

***21e**[GaCl$_4$]*. 2 h reaction time; Yield: 79% (329 mg); mp 149.2−152.1 °C; IR (KBr, 25 °C, cm^{-1}): 2985 (m), 2897 (vs), 2237 (vw), 2179 (vw), 2031 (vw), 1384 (m), 1240 (vs), 983 (m), 893 (vs), 749 (s), 638 (vw), 562 (vs), 537 (w), 436 (s); Raman (150 mW, 25 °C, cm^{-1}): 2987 (5), 2898 (24), 1384 (8), 752 (9), 563 (22), 539 (85), 529 (17), 442 (100), 398 (25), 357 (52), 346 (20), 285 (7), 250 (9), 201 (39), 155 (23), 122 (15); ^{1}H NMR (CD_2Cl_2, 25 °C, [ppm]): δ = 3.00 (3H, d, Me, $^2J_{PH}$ = 10.8 Hz); ^{13}C{^{1}H} NMR (CD_2Cl_2, 25 °C, [ppm]): δ = 32.7 (1C, m); ^{71}Ga{^{1}H} NMR (CD_2Cl_2, 25 °C, [ppm]): δ = 213 (s, $\nu_{1/2}$ = 4300 Hz); elemental analysis for $CH_3Cl_5GaP_5$ (416.89): calcd.: C 2.9, H 0.7; found: C 3.2, H 1.1; **21e**[$AlCl_4$]: 2 h reaction time; yield: 85% (318 mg); mp 144.5−145.9 °C; IR (KBr, 25 °C, cm^{-1}): 2988 (m), 2902 (w), 1384 (m), 1283 (w), 1156 (vw), 892 (vs), 750 (m), 561 (m),

dx.doi.org/10.1021/ic2013304 | Inorg. Chem. 2012, 51, 3374−3387

540 (w), 477 (s), 437 (vw); Raman (150 mW, 25 °C, cm^{-1}): 2993 (4), 2906 (16), 1387 (7), 750 (8), 559 (23), 541 (48), 437 (100), 397 (21), 361 (9), 353 (45), 281 (6), 251 (9), 204 (52), 181 (5), 130 (31); ^{1}H NMR (CD_2Cl_2, 25 °C, [ppm]): δ = 2.9 (3H, d, Me, $^{2}J_{HP}$ = 10.8 Hz); $^{13}C\{^{1}H\}$ NMR (CD_2Cl_2, 25 °C, [ppm]): δ = 32.6 (1C, m); ^{27}Al NMR (CD_2Cl_2, 25 °C, [ppm]): δ = 104 (s, $\nu_{1/2}$ = 371 Hz); elemental analysis for $CH_3Cl_5AlP_5$ (374.15): calcd. C: 3.2, H 0.8; found: C 3.6, H 1.2.

***21f**[GaCl$_4$]*. 2 h reaction time; reaction time; yield: 90% (431 mg); mp 124.3−126.0 °C; IR (KBr, 25 °C, cm^{-1}): 3100 (m), 3055 (w), 1996 (vw), 1971 (w), 1898 (w), 1810 (w), 1673 (w), 1576 (s), 1477 (m), 1431 (vs), 1385 (w), 1334 (s), 1309 (m), 1160 (w), 1097 (vs), 997 (m), 927 (vw), 746 (vs), 712 (w), 677 (s), 613 (s), 577 (vs), 543 (w), 500 (s), 447 (m); Raman (150 mW, 25 °C, cm^{-1}): 3064 (13), 1578 (17), 1162 (8), 1098 (9), 1025 (24), 997 (27), 577 (18), 559 (12), 545 (100), 502 (24), 439 (25), 392 (52), 378 (19), 355 (63), 342 (21), 307 (12), 231 (6), 217 (32), 201 (49), 152 (16), 126 (73); ^{1}H NMR (CD_2Cl_2, 25 °C, [ppm]): δ = 7.85 (2H, m, *m*-Ph), 7.94 (1H, m, *p*-Ph), 8.14 (2H, m, *o*-Ph); $^{13}C\{^{1}H\}$ NMR (CD_2Cl_2, 25 °C, [ppm]): δ = 131.0 (2C, d, *m*-Ph, $^{3}J_{CP}$ = 13.8 Hz), 131.5 (1C, m, *i*-Ph), 131.8 (2C, d, *o*-Ph, $^{2}J_{CP}$ = 12.9 Hz), 137.5 (1C, d, *p*-Ph, $^{4}J_{CP}$ = 3.5 Hz); $^{71}Ga\{^{1}H\}$ NMR (CD_2Cl_2, 25 °C, [ppm]): δ = 240 (s, $\nu_{1/2}$ = 10000 Hz); elemental analysis for $C_6H_5Cl_5GaP_5$ (478.96): calcd. C 15.1, H 1.1; found C 15.1, H 1.3; **21f**[AlCl$_4$]: 2 h reaction time; yield: 94% (410 mg); mp 119.5−121.2 °C; IR (KBr, 25 °C, cm^{-1}): 3100 (w), 3054 (vw), 1996 (vw), 1971 (vw), 1898 (vw), 1811 (w), 1672 (w), 1576 (m), 1477 (w), 1431 (s), 1385 (vw), 1334 (m), 1309 (w), 1160 (vw), 1098 (w), 1084 (s), 995 (m), 746 (vs), 712 (m), 678 (s), 613 (s), 580 (vs), 544 (s), 467 (w); Raman (150 mW, 25 °C, cm^{-1}) 3065 (12), 1558 (17), 1162 (7), 1099 (10), 1024 (20), 997 (28), 577 (20), 560 (11), 544 (100), 501 (21), 437 (25), 392 (47), 379 (35), 355 (70), 306 (12), 230 (6), 216 (30), 201 (53), 153 (5), 133 (50), 117 (17); ^{1}H NMR (CD_2Cl_2, 25 °C, [ppm]): δ = 7.85 (2H, m, *m*-Ph), 7.95 (1H, m, *p*-Ph), 8.14 (2H, m, *o*-Ph); $^{13}C\{^{1}H\}$ NMR (CD_2Cl_2, 25 °C, [ppm]): δ = 131.0 (2C, d, *m*-Ph, $^{3}J_{CP}$ = 13.7 Hz), 131.7 (1C, m, *i*-Ph), 131.8 (2C, d, *o*-Ph, $^{2}J_{CP}$ = 13.0 Hz), 137.6 (1C, d, *p*-Ph, $^{4}J_{CP}$ = 3.8 H); ^{27}Al-NMR (CD_2Cl_2, 25 °C, [ppm]): δ = 104 (s, $\nu_{1/2}$ = 130 Hz); elemental analysis for $C_6H_5Cl_5AlP_5$ (436.22): calcd. C 16.5, H 1.2; found: C 16.6, H 1.5.

***21g**[GaCl$_4$]*. 6 h reaction time; Yield: 62% (353 mg); mp 78.9−80.3 °C; IR (KBr, 25 °C, cm^{-1}): 1644 (vs), 1561 (vw), 1516 (vs), 1485 (vw), 1395 (w) 1303 (m), 1155 (w), 1115 (w), 1095 (s) 1023 (vw), 981 (vs), 762 (vw), 721 (m), 632 (vs), 589 (w), 572 (vs), 534 (w), 526 (s), 461 (s); Raman (300 mW, 25 °C, cm^{-1}): 1645 (8), 1397 (5), 861 (5), 591 (6), 575 (5), 540 (100), 461 (27), 440 (5), 404 (40), 359 (30), 344 (6), 224 (25), 183 (15), 144 (7), 126 (10), 92 (6); ^{19}F NMR (CD_2Cl_2, 25 °C, [ppm]): δ = −153.2 (2F, m, *m*-F), −134.2 (1F, m, *p*-F), −130.6 (2F, m, *o*-F); ^{13}C NMR (CD_2Cl_2, 25 °C, [ppm]): δ = 106.4 (1C, m, *i*-p-F), 138.5 (2C, d(br), *m*-Ph, $^{1}J_{CF}$ = 262 Hz), 146.4 (2C, d(br), *o*-Ph $^{1}J_{CF}$ = 260 Hz), 147.8 (1C, d(br), *p*-Ph, $^{1}J_{CF}$ = 273 Hz); $^{71}Ga\{^{1}H\}$ NMR (CD_2Cl_2, 25 °C, [ppm]): δ = 233 (s, $\nu_{1/2}$ = 10000 Hz); **21g**[AlCl$_4$]: Yield: 67% (353 mg); mp 93.4−95.5 °C; IR (KBr, 25 °C, cm^{-1}): 1643 (vs), 1515 (w), 1486 (vs), 1395 (m), 1303 (m), 1155 (w), 1116 (w), 1095 (vs), 1023 (w), 980 (vs), 722 (w), 633 (s), 589 (vw), 573 (s), 536 (vw), 526 (w), 473 (m); Raman (300 mW, 25 °C, cm^{-1}): 1646 (10), 1397 (8), 862 (6), 591 (11), 575 (8), 539 (100), 463 (34), 378 (5), 358 (35), 343 (21), 225 (25), 174 (9), 145 (10), 119 (12), 92 (9); ^{19}F-NMR (CD_2Cl_2, 25 °C, [ppm]): δ = −153.5 (2F, m, *m*-F), −134.3 (1F, m, *p*-F), −130.8 (2F, m, *o*-F); $^{13}C\{^{1}H\}$ NMR (CD_2Cl_2, 25 °C, [ppm]): δ = 106.9 (1C, m, *i*-Ph), 138.8 (2C, d(br), *m*-Ph, $^{1}J_{CF}$ = 262 Hz), 146.8 (2C, d(br), *o*-Ph, $^{1}J_{CF}$ = 260 Hz), 147.9 (1C, d(br), *p*-Ph, $^{1}J_{CF}$ = 269 Hz); ^{27}Al NMR (CD_2Cl_2, 25 °C, [ppm]): δ = 104 (s, $\nu_{1/2}$ = 470 Hz).

X-ray Data Collection and Reduction. Suitable single crystals for **21b-g**[GaCl$_4$] and **14a**·fluorobenzene were obtained by crystallization from a minimum amount of CH_2Cl_2 (**21b-g**[GaCl$_4$]) or fluorobenzene (**14a**) by *n*-hexane diffusion at −30 °C. The crystals were coated with Paratone-N oil, mounted using a glass fiber pin, and frozen in the cold nitrogen stream of the goniometer. X-ray diffraction data for all compounds were collected on a Bruker AXS APEX CCD diffractometer equipped with a rotating anode at 153(1) K using graphite-monochromated Mo$K\alpha$ radiation (λ = 0.71073 Å) with a scan width of 0.3° and variable exposure times typically between 5 and 15 s. In all cases generator settings were 50 kV and 180 mA. Diffraction data were collected over the full sphere, and the frames were integrated using the Bruker SMART[52] software package using the narrow frame algorithm. Data were corrected for absorption effects using the SADABS routine (empirical multiscan method). For further crystal and data collection details see Table 5.

Structure Solution and Refinement. Atomic scattering factors for non-hydrogen elements were taken from the literature tabulations. Structure solutions were found by using direct methods as implemented in the SHELXS-97 package[53]and were refined with SHELXL-97[54] against F^2 using first isotropic and later anisotropic thermal parameters for all non-hydrogen atoms. Hydrogen atom positions were calculated and allowed to ride on the carbon atom to which they are bonded, assuming a C−H bond length of 0.95 Å. H-atom temperature factors were fixed at 1.20 times the isotropic temperature factor of the C atom to which they are bonded. The H-atom contributions were calculated but not refined. The locations of the largest peaks in the final difference Fourier map as well as the magnitude of the residual electron densities in each case were of no chemical significance. For **21b**[GaCl$_4$] and **21e**[GaCl$_4$] the crystals were twins (twin law 1 0 0, 0 −1 0, 0 0 −1) with not quite equal components.

■ ASSOCIATED CONTENT

Ⓢ Supporting Information

Detailed information on the quantum chemical calculations and $^{31}P\{^{1}H\}$ NMR investigations of reaction mixtures of **13c,d,e,g** and $GaCl_3$ in various stoichiometries. This material is available free of charge via the Internet at http://pubs.acs.org.

■ AUTHOR INFORMATION

Corresponding Author

*E-mail: jweigand@uni-muenster.de.

Notes

The authors declare no competing financial interest.

■ ACKNOWLEDGMENTS

We gratefully acknowledge financial support from the Fonds der Chemischen Industrie (fellowships to M.H.H. and K.-O.F.), the DFG (WE 4621/2-1), the European COST network PhosSciNet (CM0802), and the International Research Training Group 1444. J.J.W. thanks Prof. F. Ekkehardt Hahn (WWU Muenster) for his support, and Prof. Robert Wolf (University of Regensburg) for helpful discussions.

■ REFERENCES

(1) (a) Baudler, M. *Angew. Chem., Int. Ed. Engl.* **1982**, *7*, 492. (b) Baudler, M. *Angew. Chem., Int. Ed. Engl.* **1987**, *26*, 419.

(2) Dyker, C. A.; Burford, N. *Chem.—Asian J.* **2008**, *3*, 28.

(3) (a) Krossing, I.; Raabe, I. *Angew. Chem., Int. Ed.* **2001**, *40*, 4406. (b) Bihlmeier, A.; Gonsior, M.; Raabe, I.; Trapp, N.; Krossing, I. *Chem.—Eur. J.* **2004**, *10*, 5041. (c) Krossing, I. *J. Chem. Soc., Dalton Trans.* **2002**, 500. (d) Gonsior, M.; Krossing, I.; Müller, L.; Raabe, I.; Jansen, M.; van Wüllen, L. *Chem.—Eur. J.* **2002**, *8*, 4475.

(4) Weigand, J. J.; Burford, N.; Decken, A. *Eur. J. Inorg. Chem.* **2008**, 4343.

(5) Weigand, J. J.; Holthausen, M. H.; Fröhlich, R. *Angew. Chem., Int. Ed.* **2009**, *48*, 295.

(6) Holthausen, M. H.; Weigand, J. J. *J. Am. Chem. Soc.* **2009**, *131*, 14210.

(7) Holthausen, M. H.; Richter, C.; Hepp, A.; Weigand, J. J. *Chem. Commun.* **2010**, *46*, 6921.

(8) (a) Alton, E. R.; Montemayor, R. G.; Parry, R. W. *Inorg. Chem.* **1974**, *13*, 2267. (b) Schultz, C. W.; Parry, R. W. *Inorg. Chem.* **1976**, *15*, 3046. (c) Kopp, R. W.; Bond, A. C.; Parry, R. W. *Inorg. Chem.* **1976**, *15*, 3042. (d) Thomas, M. G.; Schultz, C. W.; Parry, R. W. *Inorg. Chem.* **1977**, *16*, 994. (e) Shagvaleev, F. S.; Zykova, T. V.; Tarasova, R. I.; Sitdikova, T. S.; Moskva, V. V. *Zh. Obshch. Khim.* **1990**, *60*, 1775.

(9) (a) Shagvaleev, F. S.; Zykova, T. V.; Tarasova, R. I.; Sitdikova, T. S.; Moskva, V. V. *J. Gen. Chem. USSR (Engl. Trans.)* **1990**, *60*, 1585; (b) *Z. Obshch. Khim.* **1990**, *60*, 1775. (c) Burford, N.; Ragogna, P. J.; McDonald, R.; Ferguson, M. J. *J. Am. Chem. Soc.* **2003**, *125*, 14404. (d) Burford, N.; Herbert, D. E.; Ragogna, P. J.; McDonald, R.; Ferguson, M. J. *J. Am. Chem. Soc.* **2004**, *126*, 17067. (e) Burford, N.; Dyker, C. A. M.; Lumsden, M.; Decken, A. *Angew. Chem., Int. Ed.* **2005**, *44*, 6196. (f) Dyker, C. A.; Burford, N.; Lumsden, M. D.; Decken, A. *J. Am. Chem. Soc.* **2006**, *128*, 9632. (g) Weigand, J. J.; Burford, N.; Lumsden, M.; Decken, A. *Angew. Chem., Int. Ed.* **2006**, *45*, 6733. (h) Riegel, S. D.; Burford, N.; Lumsden, M. D.; Decken, A. *Chem. Commun.* **2007**, 4469. (i) Carpenter, Y.; Dyker, C. A.; Burford, N.; Lumsden, M. D.; Decken, A. *J. Am. Chem. Soc.* **2008**, *130*, 15732.

(10) Burford, N.; Ragogna, P. J. *J. Chem. Soc., Dalton Trans.* **2002**, 4307.

(11) Cowley, A. H.; Kemp, R. A. *Chem. Rev.* **1985**, *85*, 367.

(12) Michalik, D.; Schulz, A.; Villinger, A.; Weding, N. *Angew. Chem., Int. Ed.* **2008**, *47*, 6465.

(13) (a) Dumitrescu, A.; Gornitzka, H.; Schoeller, W. W.; Bourissou, D.; Bertrand, G. *Eur. J. Inorg. Chem.* **2002**, 1953. (b) Reeske, G.; Hoberg, C. R.; Hill, N. J.; Cowley, A. H. *J. Am. Chem. Soc.* **2008**, *128*, 2800. (c) Dube, J. W.; Farrar, G. J.; Norton, E. L.; Szekely, K. L. S.; Cooper, B. F. T.; McDonald, C. L. B. *Organometallics* **2009**, *28*, 4377. (d) Reed, R. W.; Xie, Z.; Reed, C. A. *Organometallics* **1995**, *14*, 5002. (e) Schmidtpeter, A.; Jochem, G.; Klinger, C.; Robl, C.; Nöth, H. *J. Organomet. Chem.* **1997**, *529*, 87.

(14) Symmes, C.; Quin, L. D. *J. Org. Chem.* **1978**, *43*, 1250.

(15) (a) Henderson, W. A. Jr.; Streuli, C. A. *J. Am. Chem. Soc.* **1960**, *82*, 5791. (b) Laurence, C.; Gal, J.-F. *Lewis Basicity and Affinity Scales: Data and Measurement*, 1st. ed.; John Wiley & Sons: London, U.K., 2010; (c) Quin, L. D. *A Guide to Organophosphorus Chemistry*, 1st. ed.; John Wiley & Sons: New York, 2000.

(16) (a) Kashman, Y.; Menachem, Y.; Benary, E. *Tetrahedron* **1973**, *29*, 4279. (b) Crews, P. *J. Org. Chem.* **1975**, *40*, 1170. (c) Kashman, Y.; Rudi, A. *Tetrahedron Lett.* **1976**, *32*, 2819. (d) Rudi, A.; Kashman, Y. *Tetrahedron Lett.* **1978**, *25*, 2209. (e) Cowley, A. H.; Stewart, C. A.; Whittlesey, B. R.; Wright, T. C. *Tetrahedron Lett.* **1984**, *25*, 815.

(17) (a) Carpenter, Y. *Investigation into the Reactivity and Structure of Phosphinophosphonium Cations and Related Species*; Ph.D. Thesis, Dalhousie University, Halifax, NS, Canada, December 2010; (b) Carpenter, Y.; Burford, N.; Lumsden, M. D.; McDonald, R. *Inorg. Chem.* **2011**, *50*, 3342.

(18) Only species are reported whose concentration in solution is significantly higher than 3% (determined by $^{31}P\{^{1}H\}$ NMR).

(19) Temperature dependent NMR investigations were not performed because of the narrow liquid phase of fluorobenzene (m.p. −42.2 °C; b.p. 96.1 °C. Ginzburg, B. M.; Tuichiev, S. *Russian J. Appl. Chem.* **2009**, *82*, 1178.

(20) Gonsior, M.; Krossing, I.; Matern, E. *Chem.—Eur. J.* **2006**, *12*, 1703.

(21) Burford, N.; Cameron, T. S.; LeBlanc, D. J.; Losier, P.; Sereda, S.; Wu, G. *Organometallics* **1997**, 4712.

(22) Norman, N. C.; Pickett, N. L. *Coord. Chem. Rev.* **1995**, *145*, 27.

(23) (a) Slattery, J. M.; Fish, C.; Green, M.; Hooper, T. N.; Jeffery, J. C.; Kilby, R. J.; Lynam, J. M.; McGrady, J. E.; Pantazis, D. A.; Russel, C. A.; Willians, C. E. *Chem.—Eur. J.* **2007**, *13*, 6967. (b) Le, T. D.; Arquier, D.; Miqueu, K.; Sotiropoulos, J.-M.; Coppel, Y.; Bastin, S.; Igau, A. *J. Organomet. Chem.* **2009**, *694*, 229.

(24) Drago, R. S.; Joerg, S. *J. Am. Chem. Soc.* **1996**, *118*, 2654.

(25) Tolman, C. A. *Chem. Rev.* **1977**, *77*, 315.

(26) Nagy, G.; Balde, D. French Patent 1950691, *Chem. Abstr.* **1967**, *67*, 3142.

(27) Frank, W.; Gelhausen, B.; Reiss, G. J.; Salzer, R. Z. *Naturforsch. B.: Chem. Sci.* **1998**, *53*, 1149.

(28) We assume that this also results from $GaCl_3$ induced Friedel–Crafts type arylation reactions.

(29) Ulvenlund, S.; Whaetley, A.; Bengtsson, L. A. *J. Chem. Soc., Dalton Trans.* **1995**, *2*, 245.

(30) Ulvenlund, S.; Bengtsson-Kloo, L.; Ståhl, K. *J. Chem. Soc., Faraday Trans.* **1995**, *91*, 4223.

(31) Gudat, D. *Eur. J. Inorg. Chem.* **1998**, 1087.

(32) Schoeller, W. W. *Phys. Chem. Chem. Phys.* **2009**, *11*, 5273.

(33) The additionally added Lewis acid ECl_3 (E = Ga, Al) lead to a significant broadening of the corresponding ^{71}Ga and ^{27}Al NMR resonances, for similar observations see ref 32.

(34) Hansch, C.; Leo, A. *Exploring QSAR: Fundamentals and Applications in Chemistry and Biology*; American Chemical Society: Washington, DC, 1995; Vols. *1* and *2*.

(35) Chang, I. S.; Price, J. T.; Tomlinson, A. J.; Willis, C. *Can. J. Chem.* **1972**, *50*, 512.

(36) Budzelaar, P. H. M. *gNMR for Windows (5.0.6.0) NMR Simulation Program*; Cherwell Scientific, 2006.

(37) (a) Taft, R. W. *J. Am. Chem. Soc.* **1952**, *74*, 2729. (b) Taft, R. W. *J. Am. Chem. Soc.* **1953**, *75*, 4231.

(38) (a) McFarlane, H. C. E.; McFarlane, W.; Nash, J. A. *Dalton Trans.* **1980**, 240. (b) Aime, S.; Harris, R. K.; McVicker, E. M.; Fild, M. *Dalton Trans.* **1976**, 2144. (c) Forgeron, M. A. M.; Gee, M.; Wasylishen, R. E. *J. Phys. Chem.* **2004**, *108*, 4895. (d) Del Bene, J. E.; Elguero, J.; Alkorta, I. *J. Phys. Chem.* **2004**, *108*, 3662.

(39) (a) Tattershall, B. W.; Kendall, N. L. *Polyhedron* **1994**, *10*, 1517. (b) Baudler, M.; Adamek, C.; Opiela, S.; Budzikiewicz, H.; Ouzounis, D. *Angew. Chem., Int. Ed.* **1988**, *27*, 1059. (c) Niecke, E.; Rüger, R.; Krebs, B. *Angew. Chem., Int. Ed. Engl.* **1982**, *21*, 544. (d) Jutzi, P.; Meyer, U. *J. Organomet. Chem.* **1987**, *333*, C18.

(40) Weigand, J. J.; Riegel, S. D.; Burford, N.; Decken, A. *J. Am. Chem. Soc.* **2007**, *129*, 7969.

(41) For values of $^{3}J_{PF}$ couplings see, e.g., (a) Westenkirchner, A.; Villinger, A.; Karaghiosoff, K.; Wustrack, R.; Michalik, D.; Schulz, A. *Inorg. Chem.* **2011**, *50*, 2691. (b) Hoge, B.; Panne, P. *Chem.—Eur. J.* **2006**, *12*, 9025.

(42) (a) Miller, G. R.; Yankowsky, A. W.; Grim, S. O. *J. Chem. Phys.* **1969**, *51*, 3185. (b) Fluck, E.; Wachtler, D. *Liebigs Ann. Chem.* **1979**, 1125.

(43) Xiong, Y.; Yao, S.; Brym, M.; Driess, M. *Angew. Chem., Int. Ed.* **2007**, *46*, 4511.

(44) (a) Niecke, E.; Rüger, R.; Krebs, B. *Angew. Chem., Int. Ed. Engl.* **1982**, *21*, 544. (b) Schoeller, W. W.; Staemmler, V.; Rademacher, P.; Niecke, E. *Inorg. Chem.* **1986**, *25*, 4382.

(45) Wolstenholme, D. J.; Weigand, J. J.; Davidson, R. J.; Pearson, J. K.; Cameron, T. S. *J. Phys. Chem. A* **2008**, *112*, 3424.

(46) Weigand, J. J.; Burford, N.; Davidson, R. J.; Cameron, T. S.; Seelheim, P. *J. Am. Chem. Soc.* **2009**, *131*, 17943.

(47) Sum of covalent radii: $r(P) = 1.10$, $r(C) = 0.77$, $r(Cl) = 0.99$; Wiberg, N.; Wiberg, E.; Hollemann, A. F. *Lehrbuch der Anorganischen Chemie*, 102nd ed.; Walter de Gruyter: Berlin, Germany, 2007; Anhang IV.

(48) Bondi, A. *J. Phys. Chem.* **1964**, *68*, 441.

(49) Henderson, A. W.; Buckler, S. A.; Day, N. E.; Grayson, M. *J. Org. Chem.* **1961**, *26*, 4770.

(50) Fild, M.; Stelzer, O.; Schmutzler, R. *Inorg. Synth.* **1973**, *14*, 4.

(51) Magnelli, D.; Tesi, G.; Lowe, J. U.; McQuiston, W. E. *Inorg. Chem.* **1966**, *5*, 457.

(52) *SMART, program package*; Bruker AXS: Madison, WI, 2000.

(53) *SHELXS-97*; Sheldrick, G. M. *Acta Crystallogr.* **1990**, *A46*, 467.

(54) Sheldrick, G. M. *SHELXL-97*; Universität Göttingen: Göttingen, Germany, 1997.